



Hawaii Coastal Seawater CO₂ Network: A Statistical Evaluation of a Decade of Observations on Tropical Coral Reefs

Gerianne J. Terlouw¹, Lucie A. C. M. Knor^{1*}, Eric Heinen De Carlo¹, Patrick S. Drupp¹, Fred T. Mackenzie¹, Yuan Hui Li¹, Adrienne J. Sutton², Albert J. Plueddemann³ and Christopher L. Sabine¹

¹ Department of Oceanography, SOEST, University of Hawai'i at Mānoa, Honolulu, HI, United States, ² Pacific Marine Environmental Laboratory, National Oceanic and Atmospheric Administration, Seattle, WA, United States, ³ Woods Hole Oceanographic Institution, Woods Hole, MA, United States

OPEN ACCESS

Edited by:

Tyler Cyronak,
University of California, San Diego,
United States

Reviewed by:

Wiley Evans,
Hakai Institute, Canada
Lester Kwiatkowski,
UMR8539 Laboratoire
de Météorologie Dynamique (LMD),
France

*Correspondence:

Lucie A. C. M. Knor
luciek@hawaii.edu

Specialty section:

This article was submitted to
Coastal Ocean Processes,
a section of the journal
Frontiers in Marine Science

Received: 31 January 2019

Accepted: 11 April 2019

Published: 07 May 2019

Citation:

Terlouw GJ, Knor LACM,
De Carlo EH, Drupp PS,
Mackenzie FT, Li YH, Sutton AJ,
Plueddemann AJ and Sabine CL
(2019) Hawaii Coastal Seawater CO₂
Network: A Statistical Evaluation of a
Decade of Observations on Tropical
Coral Reefs. *Front. Mar. Sci.* 6:226.
doi: 10.3389/fmars.2019.00226

A statistical evaluation of nearly 10 years of high-resolution surface seawater carbon dioxide partial pressure ($p\text{CO}_2$) time-series data collected from coastal moorings around O'ahu, Hawai'i suggest that these coral reef ecosystems were largely a net source of CO₂ to the atmosphere between 2008 and 2016. The largest air-sea flux ($1.24 \pm 0.33 \text{ mol m}^{-2} \text{ yr}^{-1}$) and the largest variability in seawater $p\text{CO}_2$ (950 μatm overall range or 8x the open ocean range) were observed at the CRIMP-2 site, near a shallow barrier coral reef system in Kaneohe Bay O'ahu. Two south shore sites, Kilo Nalu and Ala Wai, also exhibited about twice the surface water $p\text{CO}_2$ variability of the open ocean, but had net fluxes that were much closer to the open ocean than the strongly calcifying system at CRIMP-2. All mooring sites showed the opposite seasonal cycle from the atmosphere, with the highest values in the summer and lower values in the winter. Average coastal diurnal variabilities ranged from a high of 192 $\mu\text{atm/day}$ to a low of 32 $\mu\text{atm/day}$ at the CRIMP-2 and Kilo Nalu sites, respectively, which is one to two orders of magnitude greater than observed at the open ocean site. Here we examine the modes and drivers of variability at the different coastal sites. Although daily to seasonal variations in $p\text{CO}_2$ and air-sea CO₂ fluxes are strongly affected by localized processes, basin-scale climate oscillations also affect the variability on interannual time scales.

Keywords: time series, CO₂, reef, coastal, ocean acidification, variability, fluxes

INTRODUCTION

Since the start of the industrial revolution, atmospheric CO₂ concentrations have increased steadily from ~280 ppm in preindustrial times, reaching 408 ppm in 2018 at the Mauna Loa Observatory, Hawai'i Island, Hawai'i¹ (Keeling et al., 1976, 2001; Tans and Keeling, 2017; Dlugokencky and Tans, 2018). The average annual growth rate of atmospheric CO₂ was 2 ppm yr⁻¹ during the last decade (2007–2016), but varies from year to year (Dlugokencky and Tans, 2018). Through the process of air-sea gas exchange, the global ocean has taken up approximately one quarter of the CO₂

¹<https://www.esrl.noaa.gov/gmd/ccgg/trends/>

emissions since the Industrial Revolution (Le Quéré et al., 2018). The trend of rising atmospheric CO₂ concentrations has been well documented for several decades at various geographic locations (Keeling et al., 1976, 2001; Thoning et al., 1989; Chamard et al., 2003). Over the last 20 years, the uptake of CO₂ by the ocean, the subsequent decrease in seawater pH (Ocean Acidification, OA), and the consequences of enhanced ocean acidity for the marine environment and its organisms has been an important topic of study (Kleypas et al., 1999; Caldeira and Wickett, 2003; Feely et al., 2004; Sabine et al., 2004; Kleypas and Langdon, 2006; Hoegh-Guldberg et al., 2007; Dore et al., 2009; Gattuso and Hansson, 2011; Andersson and Gledhill, 2013; Mackenzie and Andersson, 2013).

Quantifying CO₂ fluxes in the coastal ocean and particularly in coral reef ecosystems can be more challenging than in the open ocean owing to a variety of factors, including especially the larger variability observed in the former. To help resolve this problem, high-resolution monitoring of seawater partial pressure of CO₂ ($p\text{CO}_{2\text{sw}}$) on surface buoys in coastal regions began late in 2005 (see Massaro et al., 2012). Ocean carbonate chemistry research conducted in various coastal settings (Drupp et al., 2011, 2013; Yan et al., 2011, 2016; Massaro et al., 2012; Bates et al., 2014; Shaw et al., 2014; Sutton et al., 2014a, 2016) has shown that, in order to understand the drivers of natural variability and identify long-term trends, it is necessary to gain better insight into the processes that control marine CO₂ concentrations, including the direction and magnitude of the air-sea CO₂ flux.

The high temporal variability of the CO₂-carbonate system parameters in coral reefs is associated with changes in the magnitude of forcing mechanisms, and resultant changes in other water quality parameters (Kayanne et al., 1995; Gagliano et al., 2010; Drupp et al., 2011, 2013; Hofmann et al., 2011; Shamberger et al., 2011; Price et al., 2012; Shaw and McNeill, 2014; Courtney et al., 2017). Although great strides have been made over the past few years in adding time-series stations on coral reefs, and undertaking process-based studies at these locations (e.g., Yeakel et al., 2015; Drupp et al., 2016; Courtney et al., 2017; Page et al., 2017, 2018; Eyre et al., 2018), it is only at a relatively small number of sites that the biogeochemical conditions in waters of coral reefs have been successfully observed for extended periods of time. Hence, thorough characterization and unequivocal attribution of observed changes to ocean acidification (OA) remain elusive for most coral reef settings.

The biogeochemistry of Hawai'i's coastal waters is strongly influenced by land-derived nutrient inputs (Ringuet and Mackenzie, 2005; De Carlo et al., 2007; Fagan and Mackenzie, 2007; Hoover and Mackenzie, 2009), which drive primary productivity and impact the CO₂-carbonic acid system parameters (e.g., Fagan and Mackenzie, 2007; Drupp et al., 2011, 2013; Shamberger et al., 2011; Massaro et al., 2012). High-nutrient freshwater entering coastal waters causes increased phytoplankton growth, often leading to the drawdown of $p\text{CO}_{2\text{sw}}$ (Fagan and Mackenzie, 2007; Drupp et al., 2011; Massaro et al., 2012). The duration of such phytoplankton blooms depends strongly on physical processes including water residence time and mixing (e.g., De Carlo et al., 2007;

Tomlinson et al., 2011), as well as biotic effects such as predation (e.g., Hoover et al., 2006).

In an effort to characterize the dynamics of the CO₂-carbonic acid system in waters bathing coral reefs on short and long time scales, NOAA/PMEL and University of Hawai'i scientists established the first coastal seawater $p\text{CO}_2$ monitoring station at Kaneohe Bay in 2005. The Coral Reef Instrumented and CO₂ Monitoring Platform (CRIMP-CO₂) was first deployed in southern Kaneohe Bay, but was moved in 2008 to the inner edge of the barrier reef. Two additional buoys were also deployed in 2008 on the south shore of O'ahu, Hawai'i (see **Figure 1**). A fourth buoy was added in 2011 on the off-shore side of the Kaneohe Bay barrier reef to help characterize the source waters entering the bay. The buoys collect high temporal resolution (3-hourly) CO₂ time-series data that have been used to assess inorganic carbon variability (Massaro et al., 2012; Drupp et al., 2013). These now nearly decade-long time series provide a unique opportunity to quantify the influence of local climatic, geographic, and biogeochemical processes on CO₂ dynamics. An open ocean mooring, WHOI Hawaii Ocean Time Series (WHOTS), operated by the Woods Hole Oceanographic Institution (WHOI), 100 km North of O'ahu, in the North Pacific Subtropical Gyre, also collects high-resolution surface seawater $p\text{CO}_2$ ($p\text{CO}_{2\text{sw}}$) observations and provides an open ocean reference to compare to data from the coastal O'ahu sites (Dore et al., 2003; Sutton et al., 2017). The WHOTS mooring is located at the station ALOHA (A Long-term Oligotrophic Habitat Assessment) oceanographic observatory (Karl and Church, 2018).

This paper builds on earlier work (Drupp et al., 2013) and utilizes nearly 10 years of seawater $p\text{CO}_2$ data to investigate long-term changes and differences in variability across sites around O'ahu, Hawai'i. Due to the low signal-to-noise ratio in these highly variable coastal locations, the datasets are too short to discern statistically significant long-term trends in $p\text{CO}_{2\text{sw}}$, which underscores the importance of continuing high-quality observations. Regardless, data from these stations represent the longest running coordinated autonomous $p\text{CO}_2$ time series characterizing differing coral environments around a single island. The high-resolution data permit a detailed description and analysis of the variability of $p\text{CO}_{2\text{sw}}$ in O'ahu's coastal waters. The results of this study enhance our understanding of the behavior of the tropical coastal ocean with respect to the CO₂-carbonic acid system and provide a basis to begin to refine regional coastal CO₂ budgets. Our observations and interpretation also contribute to the goals of the Global Ocean Acidification Observing Network (GOA-ON) to determine spatio-temporal patterns in carbon chemistry, and provide information for state and federal agency managers and decision makers with respect to coastal management.

MATERIALS AND METHODS

Environmental Setting

The CRIMP-2 buoy is a Moored Autonomous $p\text{CO}_2$ (MAPCO₂) buoy that was deployed in June 2008 over a sandy bottom in

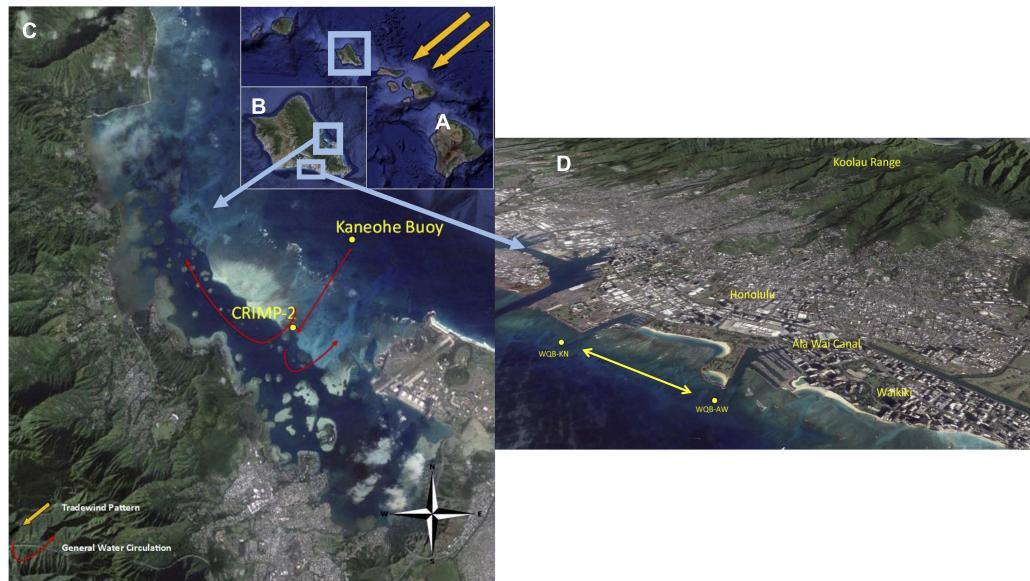


FIGURE 1 | Locations of the four O'ahu coral reef MAPCO₂ moorings. **(A)** The Hawaiian Islands, highlighting O'ahu. **(B)** The island of O'ahu, highlighting Kaneohe Bay on the windward (east) coast and the Honolulu watersheds on the southern coast. **(C)** Kaneohe Bay, with the CRIMP-2 buoy located on the back reef and the Kaneohe buoy on the deeper forereef. The red dot represents the previous CRIMP location. **(D)** Two south shore buoys, Ala Wai (WQB-AW) and Kilo Nalu (WQB-KN) are located 200 m offshore of urban Honolulu above fringing reefs. WQB-AW is located near the mouth of the Ala Wai Canal, which drains the Honolulu city watersheds. Adapted from Drupp et al. (2013).

three meters of water depth on the landward edge of the barrier reef of Kaneohe Bay (**Figure 1**). Kaneohe bay is the largest semi-enclosed water body on O'ahu and is located on the windward side of the island, where northeasterly trade winds blow most of the year (Giambelluca et al., 1986, 2011). The entire bay is relatively shallow, with a mean depth of 9.5 m. The depth of the barrier reef is quite variable with a significant area characterized by approximately 2 m water depth, and the mean tidal amplitude in the bay is 68 cm (Ringuet and Mackenzie, 2005). Water at the CRIMP-2 location has a variable residence time (hours to days: Lowe et al., 2009a,b; Ho et al., 2019), which is long compared to the two buoy locations on the South Shore of O'ahu. Generally, open ocean water crosses the barrier reef before reaching CRIMP-2, then enters the deeper lagoon and returns to the ocean through the shallow Sampan Channel (Lowe et al., 2009a,b). A fraction of the water, however, does not complete its trajectory across the reef and advects toward the Sampan channel, complicating exact residence time estimates (Courtney et al., 2017). Subsequently some of the water exiting the bay during outgoing tides is recirculated over the barrier reef, the amount depending on wind strength and direction and wave conditions.

Two other MAPCO₂ buoys, Ala Wai and Kilo Nalu, are located on sand patches within the spur and groove structure of fringing reefs offshore of Honolulu, in Mamala Bay on the South Shore of O'ahu (**Figure 1**). Compared to the CRIMP-2 location, this coastline is unprotected. It is directly affected by tides and winds, and is exposed to open ocean swells from the south, particularly during the Austral winter. The Ala Wai buoy (WQB-AW in **Figure 1**) is ~300 m offshore of the mouth of the Ala Wai Canal, where freshwater discharge from a large part

of urban Honolulu often delivers high nutrient and sediment loads to the buoy site (e.g., De Carlo et al., 2004; Tomlinson et al., 2011). The Kilo Nalu buoy (WQB-KN in **Figure 1**), located ~400 m offshore, is not directly affected by stream discharge, although the local coastal waters receive urban overland runoff, input from nearby storm drains, and groundwater discharge. Depending on currents and wind conditions, some water from the Ala Wai canal occasionally advects toward the Kilo Nalu site. Water on the south shore fringing reefs is thought to have a short residence time because of significant tidal and wind-driven currents. Near bed current velocities at Kilo Nalu of nearly one knot have been reported (Fogaren et al., 2013). Stronger values are typically observed near the surface, particularly during rising tides, when the flow is in the same direction as the predominant wind driven flow. Data coverage for the 8-year record for all Hawaii sites ranged from 40% (Ala Wai) to 77% (CRIMP-2) for $p\text{CO}_{2\text{sw}}$. Data gaps were due to time spent off station for annual servicing and sensor/platform malfunctions.

The WHOTS buoy is the surface element of an open ocean mooring, located within the Station ALOHA circle, centered at 22° 45' N, 158° W approximately 100 km due north of O'ahu in the oligotrophic North Pacific Ocean². A MAPCO₂ system on the WHOTS buoy has provided a continuous time series since 2004, complementing the Hawai'i Ocean Time Series (HOT) ship-based program that has been operating at Station ALOHA for more than 25 years. OA and the fluxes of CO₂ have been well characterized at the HOT site (Dore et al., 2003, 2009; Sutton et al., 2017).

²<http://uop.whoi.edu/currentprojects/whots/whots.html>

To put the findings of this study in a more global context, the CRIMP-2 seawater $p\text{CO}_2$ time-series data from three other coral reef MAPCO₂ sites³ are directly compared. Two are located in the Atlantic Ocean (“La Parguera” in Puerto Rico, and “Crescent reef” in Bermuda) and one is in the Pacific (“Chuuk K1” in Micronesia). These three sites were chosen mainly because of their relatively long and continuous CO₂ record and their different geographic locations. La Parguera and Crescent reef are both located in the North Atlantic Ocean. Crescent reef in Bermuda is a high latitude reef (32.40°N, 64.79°W), where the large seasonal sea surface temperature (SST) cycle drives the observed large seasonal $p\text{CO}_2$ cycle. The La Parguera site in Puerto Rico (17.95°N, 67.05°W) is located within a natural reserve on a shallow (1.5–5 m) fore-reef. Chuuk K1 in the equatorial Pacific is a low latitude (7.46°N, 151.90°E) reef located in Micronesia within a semi- enclosed atoll in ~23 m water depth. Time frames evaluated were 2009–2016 for La Parguera, 2011–2016 for Chuuk-K1, and 2010–2016 for Crescent reef.

Measurements

At the above described locations, a MAPCO₂ system is deployed on each of the surface buoys. The MAPCO₂ measures the mole fraction of CO₂ ($x\text{CO}_2$) in the marine boundary layer and in air in equilibrium with surface seawater every 3 h using a non-dispersive infrared (NDIR) sensor, which is calibrated with standard reference gasses *in situ* before each measurement. The $p\text{CO}_2$ of air and seawater is calculated from the $x\text{CO}_2$ following the method of Weiss and Price (1980) with a resulting uncertainty of $< 2 \mu\text{atm}$ [see Sutton et al. (2014b) for a more detailed description of the MAPCO₂ methodology]. Other water property data including sea surface temperature (SST), salinity (SSS), dissolved oxygen (DO), turbidity and fluorescence are collected by SeaBird 16V2 instruments at the same (or higher) frequency as the CO₂ observations. Finalized quality-controlled data from the buoys are publicly available and can be found online⁴.

Ancillary Data

Wind data needed for CO₂ flux calculations at coastal locations were obtained from the NOAA-National Ocean Service Station OOUH1 in Honolulu, at the Hawai’i Institute for Marine Biology weather station on Moku o Lo’e (Coconut Island) in South Kaneohe Bay, and at the Kaneohe MCAS ID911760 (Kaneohe Marine Corps Base). Wind data for the WHOTS buoy are collected on site by an Air-Sea Interaction Meteorology (ASIMET) system (Weller, 2018).

Climate oscillation index data for the Pacific Decadal Oscillation (PDO) and the Oceanic Niño Index (ONI) were obtained from NOAA^{5,6} and for the North Pacific Gyre Oscillation from E. Di Lorenzo (Di Lorenzo et al., 2008; Chhak and Di Lorenzo, 2009)⁷.

³<https://www.pmel.noaa.gov/co2/story/Coral+Reef+Moorings>

⁴https://www.nodc.noaa.gov/ocads/oceans/time_series_moorings.html

⁵<https://www.ncdc.noaa.gov/teleconnections/pdo/>

⁶http://origin.cpc.ncep.noaa.gov/products/analysis_monitoring/ensostuff/ONI_v5.php

⁷<http://www.o3d.org/npgo/npgo.php>

Calculations

Air-sea CO₂ fluxes are calculated from the gas transfer (piston) velocity using the parameterization of Ho et al. (2006) and the sea-air $p\text{CO}_2$ difference (e.g., Weiss, 1974; Liss, 1983; Wanninkhof, 1992) according to equation (1):

$$F = k \alpha \Delta p\text{CO}_2 \quad (1)$$

where k is the gas transfer (piston) velocity, α is the solubility of CO₂ in seawater at a specified salinity and temperature, and $\Delta p\text{CO}_2$ is the difference between seawater and air $p\text{CO}_2$. The gas transfer velocity, k , was calculated using equation (2) (Ho et al., 2006):

$$k(600) = 0.266 (U10)^2 \quad (2)$$

where $k(600)$ is a scaling factor for the gas transfer velocity and $U10$ is the wind speed at 10 m altitude above the water surface. If wind speed was not measured at 10 m, it was converted to $U10$ using the wind profile power law (equation 3, Peterson and Hennessey, 1978):

$$U10 = \left(\frac{10}{z} \right)^{(1/7)} \quad (3)$$

where in (3), z is the altitude of the wind speed measurement and $1/7$ is a scaling factor that is used when assuming neutral stability conditions of the overlying atmosphere. Wind speed data were provided as hourly average values, and each wind speed value was matched with the closest buoy $p\text{CO}_2$ measurement. The uncertainty in the flux (1 standard deviation) was calculated by error propagation of $2 \mu\text{atm}$ uncertainty in the $p\text{CO}_2$ measurement (Sutton et al., 2014b) and an uncertainty of 0.019 in the gas transfer velocity, k (Ho et al., 2006). Other studies have described uncertainties in coastal CO₂ flux estimates due to the physical differences between nearshore and open ocean wind and current stresses (e.g., Tokoro et al., 2014). Although the gas transfer velocity is derived from an open ocean relationship, recent work by Ho et al. (2019) in Kaneohe Bay show its general applicability to coastal and lagoon waters. Further refinement of the gas exchange at shallow reef sites, however, would benefit from inclusion of the effect of current induced turbulence on k .

In order to isolate $p\text{CO}_2$ changes due to biogeochemical and physical factors from the direct temperature effect on solubility, the observed values were normalized to the mean temperature at each buoy over the full study period, using equation 4 (Takahashi et al., 1993, 2002). This methodology assumes that for every degree Celsius increase in temperature, the $p\text{CO}_2\text{sw}$ will increase by 4.23%.

$$p\text{CO}_2\text{sw at } T_{\text{mean}} = p\text{CO}_2\text{obs} * \exp(0.0432 * (T_{\text{mean}} - T_{\text{obs}})) \quad (4)$$

where in (4), T is the temperature in °C and the subscripts “mean” and “obs” refer to the annual mean and the individual observed values, respectively.

To plot weekly (monthly) means in averaged time series graphs, a moving average filter was applied over 56 (243) data points, which is the number of measurements made per week

(month). Additionally, monthly means were calculated for each month of the study period, and “sub-monthly” variability (mostly diurnal and tidal fluctuation) was defined as the average of the standard deviations of the monthly means. Monthly means were then averaged over each year (to annual means), and “sub-annual” variability (mostly seasonal fluctuation) was defined as the average of the standard deviations of the annual means. Finally, annual means were averaged over two 4-year periods, and the standard deviation of these means was denoted “sub-decadal” variability, describing inter-annual changes.

Long-term trends were quantified using a linear least squares regression of monthly mean $p\text{CO}_2$ values over time, with beginning and end points chosen in the same month, to avoid biases resulting from different phases of the seasonal cycle. Trend significance was calculated by doing a two sample T -test between the time series and the linear regression using a 5% significance level.

RESULTS

Seawater $p\text{CO}_2$

Descriptive statistics of $p\text{CO}_2\text{sw}$ at each site for the period from June 2008 through December 2016 are shown in **Table 1**. Mean (± 1 standard deviation of the mean) of $p\text{CO}_2\text{sw}$ values at CRIMP-2, Ala Wai, Kilo Nalu, and WHOTS were 457 ± 91 , 399 ± 29 , 386 ± 21 , and 378 ± 13 μatm , respectively. Mean $p\text{CO}_2\text{sw}$ values at Kilo Nalu and WHOTS were equal within one standard deviation, although the range in $p\text{CO}_2\text{sw}$ at Kilo Nalu was nearly twice as large as that at the open ocean WHOTS buoy (**Table 1**). The largest range in $p\text{CO}_2\text{sw}$ was observed at the CRIMP-2 buoy on the barrier reef of Kaneohe Bay, with an overall range of 950 μatm , which is nearly four times larger than the ranges at Ala Wai and Kilo Nalu (240 μatm , and 198 μatm , respectively) and about eight times the range of $p\text{CO}_2\text{sw}$ observed at the WHOTS buoy (94 μatm). Additionally, the mean daily range in $p\text{CO}_2\text{sw}$ at CRIMP-2 (**Table 2**) was nearly four times as large as at Ala Wai and Kilo Nalu, and more than an order of magnitude greater than that at WHOTS.

The time-series of $p\text{CO}_2\text{sw}$ at the four O’ahu locations, from June 2008 through December 2016, is shown in **Figure 2A**. The greatest daily variations in $p\text{CO}_2\text{sw}$ occurred at the CRIMP-2

buoy (green) while the smallest were at the WHOTS buoy (blue). A seasonal pattern was observed at all buoys, with generally higher $p\text{CO}_2\text{sw}$ in summer (May through October) than in winter (November through April). A clear deviation from the seasonal pattern is visible at Ala Wai during the period October 2013–April 2014, with $p\text{CO}_2\text{sw}$ increasing at Ala Wai, while decreasing at the other buoys. An opposite seasonal pattern was observed for atmospheric $p\text{CO}_2$ ($p\text{CO}_2\text{air}$), which is largely due to the large terrestrial carbon uptake (release) by vegetation during Northern Hemisphere summer (winter) (Keeling et al., 1976).

The $p\text{CO}_2\text{sw}$ normalized to the overall mean seawater temperature at each buoy ($p\text{CO}_2$ at T_{mean} , shown in **Figure 2B**) illustrates variations in $p\text{CO}_2\text{sw}$ presumably due primarily to biological processes (Takahashi et al., 2002). Although the sub-seasonal variations are similar to the *in situ* data, the seasonal cycle due to temperature variations is dampened, as previously described by Drupp et al. (2013).

Long term trends are more readily visualized by plotting weekly mean $p\text{CO}_2\text{sw}$ (**Figure 3**). $p\text{CO}_2\text{sw}$ was increasing at CRIMP-2 between 2012 and 2015, from a maximum weekly mean of 480 μatm in summer 2011, to a maximum of 660 μatm in summer 2014, and a slightly lower maximum of 638 μatm in September 2015. This steep increase in $p\text{CO}_2\text{sw}$ was not observed at the other buoys. **Figure 3B** also shows weekly mean $p\text{CO}_2$ at T_{mean} , with steeply increasing $p\text{CO}_2$ at Ala Wai during the winter of 2013/2014, in contrast to decreasing $p\text{CO}_2$ at T_{mean} at the other buoys during that period.

The coral reef MAPCO₂ sites from our study all display increasing $p\text{CO}_2\text{sw}$ over time [7.5 ± 1.9 (1σ), 8.3 ± 1.0 , and 2.6 ± 0.7 $\mu\text{atm yr}^{-1}$ at CRIMP-2, Ala Wai, and Kilo Nalu, respectively, **Figure 3A**]. These trends are not statistically significant for $p < 0.05$ (n.s.).

Air-Sea Fluxes of CO₂

The magnitude of instantaneous air-sea CO₂ fluxes (**Figure 4**) is much greater at the CRIMP-2 buoy than at the South Shore buoys Ala Wai and Kilo Nalu. The larger (positive as well as

TABLE 1 | Descriptive statistics for seawater $p\text{CO}_2$ ($p\text{CO}_2\text{sw}$) at CRIMP-2, Ala Wai, Kilo Nalu, and WHOTS for the entire study period.

$p\text{CO}_2\text{sw}$ (μatm)	Min	Max	Mean	Standard Deviation	Range	Mean
						Diurnal Range
CRIMP-2	196	1146	457	91	950	192
Ala Wai	298	539	399	29	240	49
Kilo Nalu	311	509	386	21	198	31
WHOTS	344	438	378	13	94	5

Range is defined as minimum – maximum of the entire study period. Diurnal range is defined as the maximum – minimum within a diurnal cycle.

TABLE 2 | Year to year air-sea CO₂ fluxes ($\text{mol C m}^{-2} \text{yr}^{-1}$) at CRIMP-2, Ala Wai, Kilo Nalu, and WHOTS buoys.

Air-Sea CO ₂ flux ($\text{mol C m}^{-2}\text{yr}^{-1}$)	CRIMP-2	Ala Wai	Kilo Nalu	WHOTS
Jun08–May09	0.76	0.00	–0.03	–0.34
Jun09–May10	0.89	0.02	0.01	N/A
Jun10–May11	1.34	0.03	0.03	–0.41
Jun11–May12	1.04	0.08	–0.05	0.51
Jun12–May13	1.23	0.04	0.01	0.07
Jun13–May14	1.51	0.15	–0.01	0.27
Jun14–May15	1.89	0.02	0.02	0.11
Jun15–May16	1.38	N/A	0.01	–0.08
Overall	1.24	0.05	0.00	0.04

CO₂ fluxes are calculated from June of one year to May of the following year, because our data set starts in June 2008. Negative values indicate sink behavior (invasion of CO₂ into seawater) and positive values indicate source behavior (outgassing of CO₂ to the atmosphere).

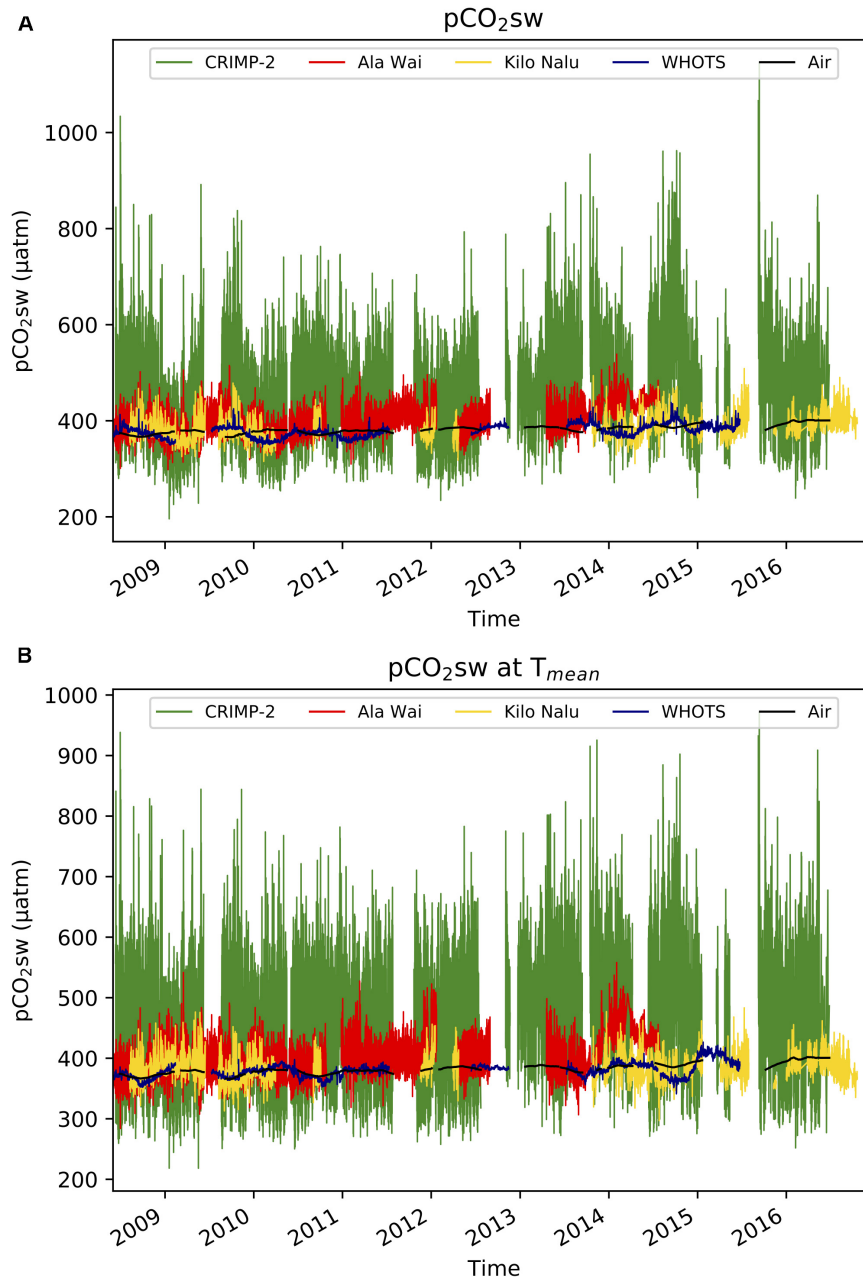


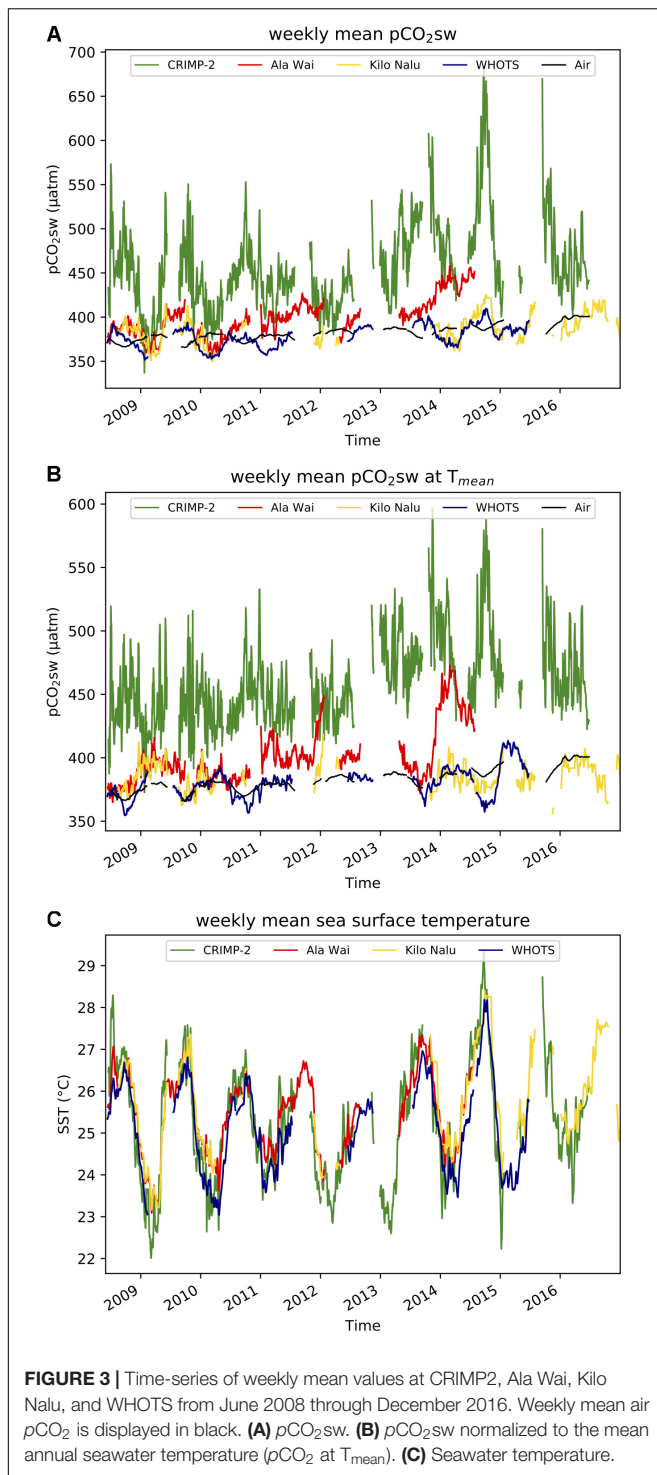
FIGURE 2 | Time-series of *in situ* (3-hourly) $p\text{CO}_{2\text{sw}}$ in μatm at CRIMP2, Ala Wai, Kilo Nalu, and WHOTS from June 2008 to December 2016. Weekly mean air $p\text{CO}_{2}$ at CRIMP2 is displayed in black. **(A)** $p\text{CO}_{2\text{sw}}$ at all sites. **(B)** $p\text{CO}_{2\text{sw}}$ normalized to the mean annual seawater temperature ($p\text{CO}_{2}$ at T_{mean}).

negative) fluxes observed at the two South Shore sites in January and March 2009 coincided with storm events (see Tomlinson et al., 2011). The annual air-sea CO₂ fluxes at each buoy from June of a given year to May of the next (Table 2), are typically an order of magnitude larger at CRIMP-2 than at either south shore buoy. The annual CO₂ flux at Ala Wai is very small but positive, while at Kilo Nalu it is negative for three out of the 8 years. The CRIMP-2 location frequently switches between CO₂ source and sink behavior, but the net annual flux over the entire study period (flux estimate ± 1 standard deviation propagated error)

at CRIMP-2 is positive ($1.24 \pm 0.33 \text{ mol m}^{-2} \text{ yr}^{-1}$; Table 2) and much larger than the fluxes of 0.05 ± 0.02 and $0.00 \pm 0.03 \text{ mol m}^{-2} \text{ yr}^{-1}$ at Ala Wai and Kilo Nalu, respectively.

Climatology

Box plots of monthly climatological $p\text{CO}_{2\text{sw}}$ and air-sea CO₂ fluxes are presented in Figures 5, 6, respectively. Although $p\text{CO}_{2\text{sw}}$ ranges from 196 to 1146 μatm at CRIMP-2 (Table 1), 99.3% of the observed values are between approximately 220 and



790 μatm . The monthly climatological mean $p\text{CO}_2\text{sw}$ at CRIMP-2 is higher and the range is slightly larger in the summer than in the winter. A much narrower range of $p\text{CO}_2\text{sw}$ is observed at the south shore buoys (298–539 μatm at Ala Wai, 311–509 μatm at Kilo Nalu, **Table 1**), and 99.3% of the $p\text{CO}_2\text{sw}$ values fall between 300 and 500 μatm at Ala Wai and between 320 and 450 μatm at Kilo Nalu.

The coral reef sites described here display a different extent of variability in $p\text{CO}_2\text{sw}$ during different months. At CRIMP-2, the highest $p\text{CO}_2\text{sw}$ and greatest variability is observed during the summer (May through October). In contrast, the most variable periods at Ala Wai occur during winter, especially in December through January. The $p\text{CO}_2\text{sw}$ at Kilo Nalu exhibits consistently less variability than Ala Wai.

Instantaneous air-sea CO₂ fluxes (**Figure 6**) also show a slight seasonal pattern similar to that of $p\text{CO}_2\text{sw}$. At CRIMP-2, higher mean fluxes are observed during summer than winter, and the lowest variability in fluxes is observed during December.

DISCUSSION

To assess various drivers of variability on selected Hawaiian reefs, we compare $p\text{CO}_2\text{sw}$ (see Variability in $p\text{CO}_2\text{sw}$) and air-sea CO₂ fluxes (see Variability in Air-Sea Fluxes) of our most open ocean-like coastal MAPCO₂ buoy, Kilo Nalu, to the offshore reference WHOTS mooring, and subsequently examine local differences between all three coral reef locations, as well as monthly climatological values.

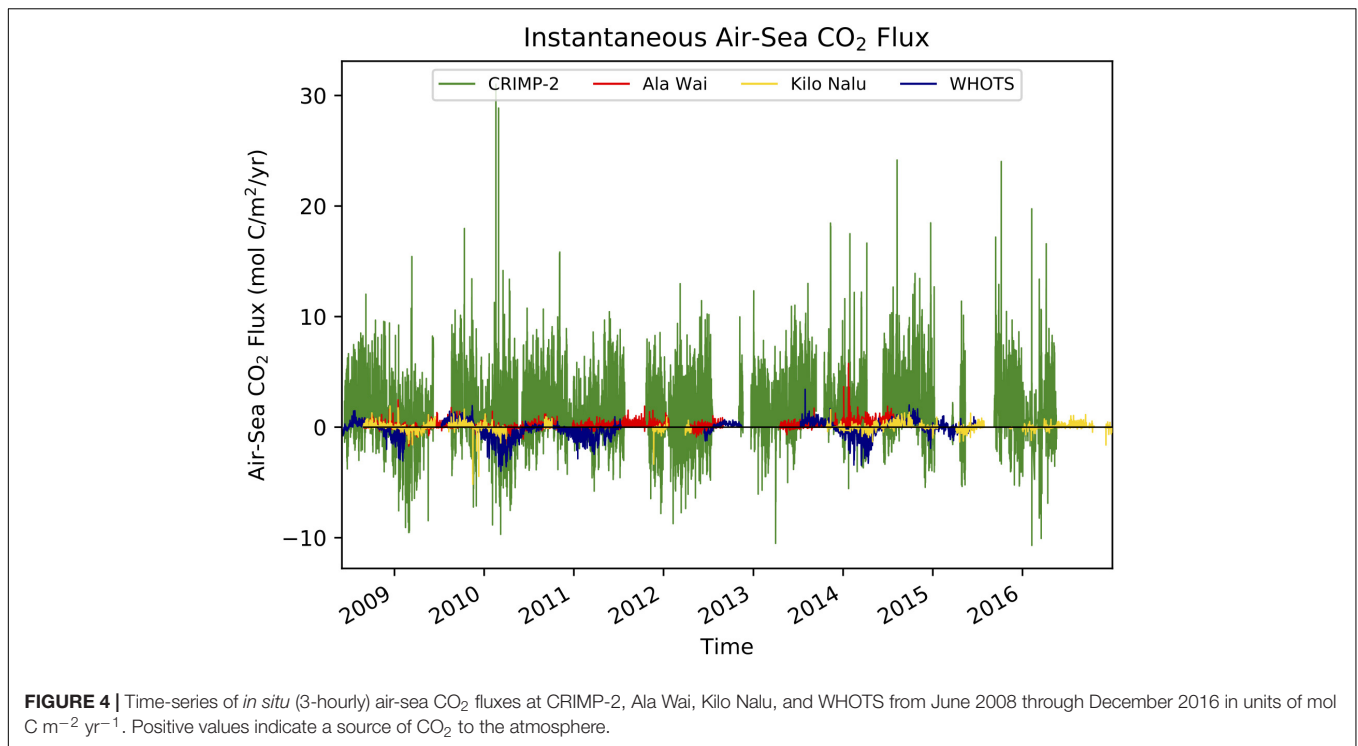
Variability in $p\text{CO}_2\text{sw}$

Coastal vs. Open Ocean $p\text{CO}_2\text{sw}$

Kilo Nalu was originally selected as a coastal reference point that should reflect near open ocean waters with well mixed conditions. There are indeed similar trends in seasonal variability in $p\text{CO}_2\text{sw}$ at Kilo Nalu and WHOTS (**Figure 7A**), which can largely be attributed to comparable seasonal SST changes at both sites. Daily $p\text{CO}_2\text{sw}$ fluctuations, however, are much greater at Kilo Nalu's coastal reef ecosystem than in the open ocean. These diurnal variations in $p\text{CO}_2\text{sw}$ at Kilo Nalu are mainly driven by greater benthic and water column photosynthesis and respiration, which reflect both the presence of a coral reef at Kilo Nalu, and the effect of discharge of nutrients and suspended solids on biogeochemical processes in proximity to land, with additional effects of calcification and dissolution on the reef (Tomlinson et al., 2011; Drupp et al., 2013). Consequently, the seasonal cycles of $p\text{CO}_2\text{sw}$ in both a nearshore reef and the open North Pacific Ocean are similar in amplitude and driven by the temperature effect on CO₂ solubility, while short-term variability is much larger in the coral reef environment largely due to biological processes.

Local Drivers of $p\text{CO}_2\text{sw}$

Local geography, weather, and proximity to land all affect $p\text{CO}_2\text{sw}$ at coastal coral reef sites. Ala Wai and Kilo Nalu buoys are both a few hundred meters from shore, moored in waters with the same depth. They differ, however, with respect to riverine input. The Ala Wai site receives direct runoff from the Ala Wai Canal, that usually does not strongly impact the Kilo Nalu buoy (Tomlinson et al., 2011). Consequently, the overall range of $p\text{CO}_2\text{sw}$ on diurnal to seasonal time scales (**Table 1**) is substantially greater at Ala Wai than those observed at Kilo Nalu (**Figures 4, 6**).



An unusual increase in $p\text{CO}_{2\text{sw}}$ at the Ala Wai buoy was observed during the winter of 2013–2014 (**Figure 3A**). A decrease in seawater temperature during the winter, however, is expected to cause a decrease in the $p\text{CO}_{2\text{sw}}$ (e.g., Takahashi et al., 1993; Massaro et al., 2012; Drupp et al., 2013). Despite the somewhat elevated seawater temperature at both south shore buoys during this period, higher $p\text{CO}_{2\text{sw}}$ values were not observed at Kilo Nalu. In the temperature-normalized $p\text{CO}_{2\text{sw}}$ record for this period (**Figure 3B**, e.g., Takahashi et al., 1993, 2002), the $p\text{CO}_{2\text{sw}}$ increase at the Ala Wai buoy is even more apparent. Consequently, it is likely that there was increased respiration and organic matter degradation at the mouth of the Ala Wai Canal during this period. This biological activity was potentially triggered by riverine runoff, as suggested by the Kilo Nalu buoy's lack of a response to direct inputs from the Ala Wai Canal.

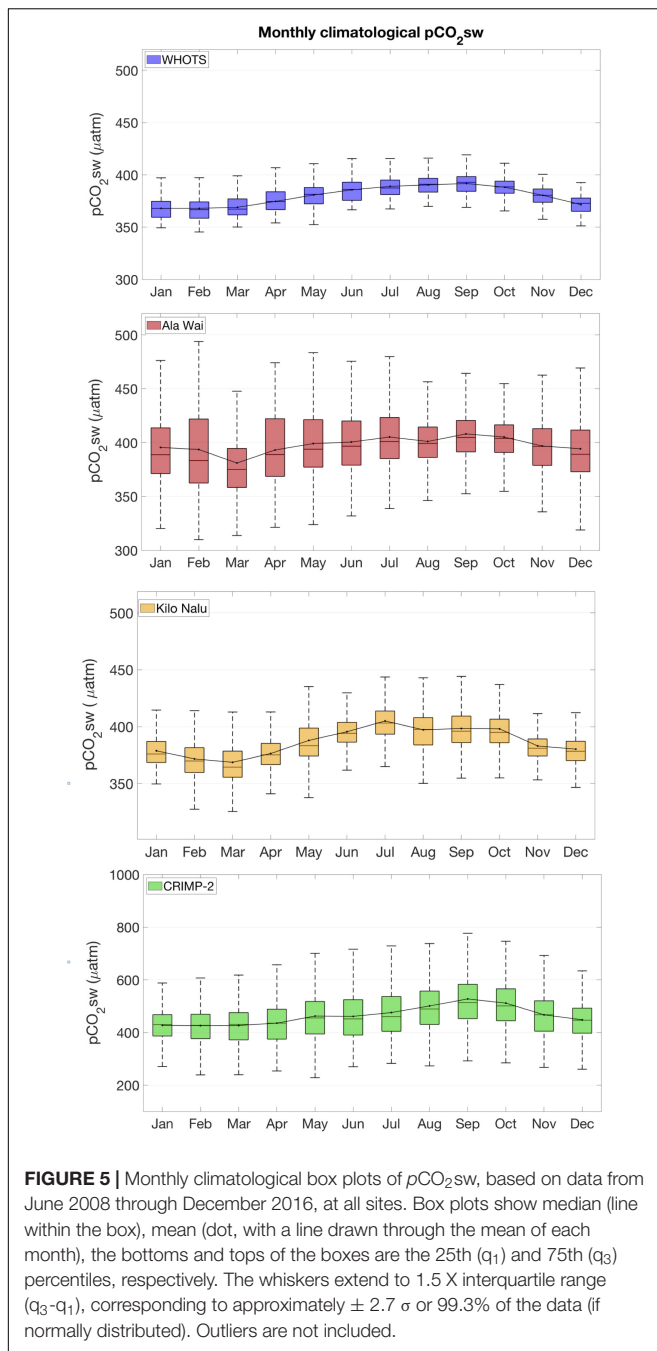
A distinguishing feature of the CRIMP-2 site is its extreme variability in $p\text{CO}_{2\text{sw}}$ compared to the South Shore buoys (**Figures 2, 4–6**). CRIMP-2 is located in shallow water (<3 m) on the inside edge of the highly productive barrier reef of Kaneohe Bay, and vigorous calcification/dissolution and primary production/respiration on the reef flat (e.g., Shamberger et al., 2011; Courtney et al., 2017) cause large and occasionally extreme daily swings in $p\text{CO}_{2\text{sw}}$. Page et al. (2018) found that organic carbon cycling (P/R) was dominating Kaneohe Bay barrier reef metabolism compared to inorganic carbon cycling (calcification/dissolution), especially in the winter, with very low $p\text{CO}_{2\text{sw}}$ due to primary productivity during the day, and a strong respiration signal leading to high $p\text{CO}_{2\text{sw}}$ at night. In addition, two physical factors result in a very large amplitude of these daily swings at CRIMP-2 compared to other coral reef sites in

this study, residence time and water depth. The longer residence time of seawater on the barrier reef of Kaneohe Bay (up to several days, Lowe et al., 2009) relative to the Honolulu sites allows for a more pronounced signature of changes in CO₂ in the water column at CRIMP-2: the products of biological reactions have a longer time to accumulate in a given parcel of water. Additionally, the shallow depth (i.e., low volume of water) at CRIMP-2 may also enhance the effects of benthic productivity and carbonate mineral-seawater interactions (e.g., Drupp et al., 2016; Page et al., 2018) on the $p\text{CO}_{2}$ of surface seawater at this location, by reducing the effective volume of water into which accumulate this and other chemical constituents associated with metabolism.

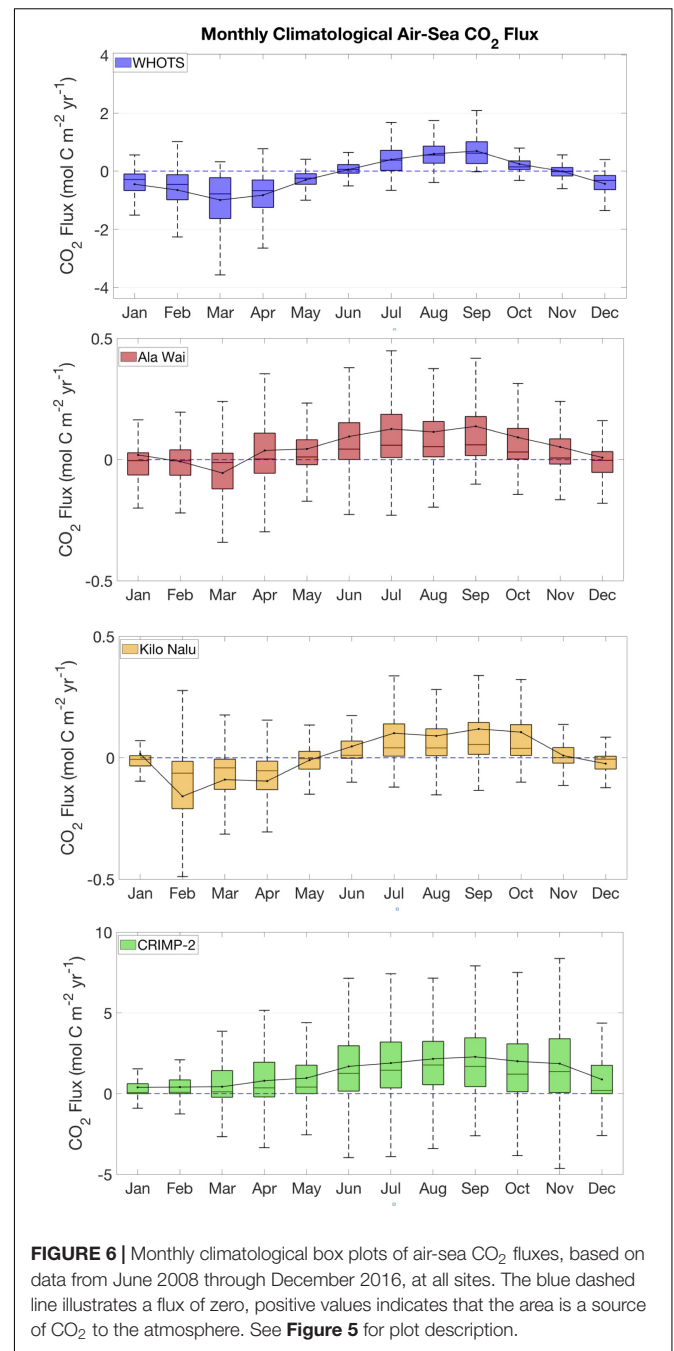
Monthly $p\text{CO}_{2\text{sw}}$ Climatology

The monthly $p\text{CO}_{2\text{sw}}$ climatology for the O'ahu coastal and WHOTS buoys (**Figure 5**) is characterized by a clear seasonal trend with lower mean $p\text{CO}_{2\text{sw}}$ during winter months and higher mean $p\text{CO}_{2\text{sw}}$ during summer months. The range of the variability (illustrated by the size of the boxes and length of the whiskers of the box plots) differs between sites, and over time at each site, reflecting how differences in physical and biogeochemical processes influence CO₂ dynamics.

At CRIMP-2, higher SST and increased productivity/respiration cycles during the summer (May through October) result in higher $p\text{CO}_{2\text{sw}}$ and greater fluctuations of $p\text{CO}_{2\text{sw}}$. Higher seawater temperature causes decreased CO₂ solubility, which increases the $p\text{CO}_{2\text{sw}}$. Productivity is enhanced by elevated seawater temperature during summer, and likely also by increased solar radiation, but this factor works in the opposite direction (CO₂ drawdown). Lower and less



variable $p\text{CO}_2\text{sw}$ during the winter months results from lower seawater temperature, lower insolation, and the concomitant effects on productivity/respiration and calcification/dissolution cycles. As mentioned earlier, the shallow depth and the relatively long residence time of water on the barrier reef of Kaneohe Bay allow for a pronounced accumulation (or depletion) of CO₂ in a given parcel of water from vigorous reef metabolism. The changes in $p\text{CO}_2\text{sw}$ due to reef metabolism are most apparent during the summer, when wind speeds are often lower and gas exchange with the atmosphere is consequently diminished.



At the South Shore buoys, Ala Wai and Kilo Nalu, the $p\text{CO}_2\text{sw}$ variability is considerably smaller than that at CRIMP-2 year-round. This reflects the less productive environment as well as the shorter water residence time and deeper water at the two fringing reef sites. At Ala Wai, $p\text{CO}_2\text{sw}$ variability is somewhat greater during the winter months. This is likely due to increased rainfall leading to more runoff of nutrients and organic matter from the Ala Wai Canal, thereby enhancing productivity during the wet season. The monthly means and the seasonal cycles at Ala Wai and Kilo Nalu are similar, but the smaller variability during the rainy season at Kilo Nalu reflects the lack of direct riverine input

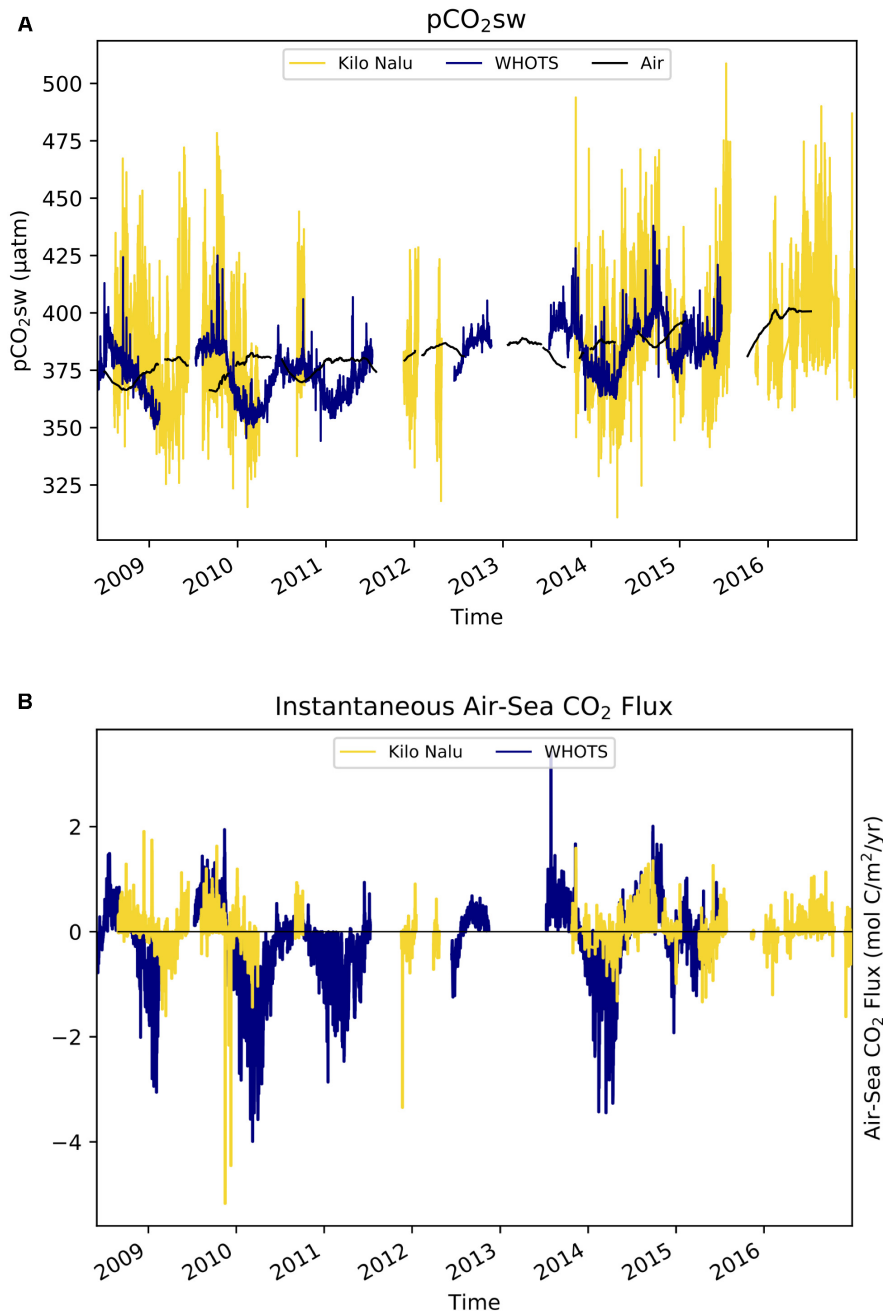


FIGURE 7 | Time-series of $p\text{CO}_{2\text{sw}}$ and air-sea CO_2 fluxes at Kilo Nalu and WHOTS from June 2008 through December 2016. This figure is similar to **Figures 2A, 4**, but plotted on a narrower y -axis range to highlight the differences in variability at Kilo Nalu and WHOTS. **(A)** *In situ* (3-hourly) $p\text{CO}_{2\text{sw}}$ in units of μatm . **(B)** Air-sea CO_2 fluxes in units of $\text{mol C m}^{-2} \text{yr}^{-1}$ where positive values indicate a source of CO_2 to the atmosphere.

at this site. The $p\text{CO}_{2\text{sw}}$ in the open ocean (WHOTS) shows little variability throughout the year.

Variability in Air-Sea Fluxes

Coastal vs. Open Ocean Air-Sea CO_2 Fluxes

Although the air-sea CO_2 fluxes at Kilo Nalu and WHOTS are more similar than their $p\text{CO}_{2\text{sw}}$ time series (**Figure 7B**), the dynamics driving these fluxes differ between locations. The

magnitude and direction of the instantaneous air-sea flux of CO_2 depend primarily on the sea-air $p\text{CO}_2$ difference ($\Delta p\text{CO}_2$) and the wind speed. Larger $p\text{CO}_{2\text{sw}}$ fluctuations at Kilo Nalu due to the biogeochemical processes described above result in larger values of $\Delta p\text{CO}_2$ as well as greater variability of $\Delta p\text{CO}_2$ than observed at WHOTS. Annual median wind speeds at Kilo Nalu (2.2 ms^{-1}) are typically lower than at WHOTS (7.5 ms^{-1}), further increasing the relative importance of the $\Delta p\text{CO}_2$ term

in the flux equation for the Kilo Nalu coastal site. Storm events can enhance the biogeochemical processes driving $\Delta p\text{CO}_2$ at Kilo Nalu, which often increases fluxes significantly. During and after storm events, Kilo Nalu is often exposed to diluted freshwater discharges of nutrients and suspended solids that are advected from the mouth of the Ala Wai canal (see Tomlinson et al., 2011, and **Figure 1**). For example, immediately after a storm that took place on March 13, 2009 (Tomlinson et al., 2011), instantaneous flux values reached a maximum of $-5.43 \text{ mol C m}^{-2} \text{ yr}^{-1}$ at the Kilo Nalu buoy. This large ocean uptake can be attributed to a seawater CO₂ drawdown associated with a phytoplankton bloom (Drupp et al., 2013). Despite these events, the net CO₂ flux throughout the full study period at Kilo Nalu is near zero, because the daily positive and negative fluxes due to biogeochemical processes mostly cancel out.

Because wind speeds at WHOTS are approximately four-fold greater than at Kilo Nalu, even the very small $\Delta p\text{CO}_2$ driven by weaker daily photosynthesis/respiration and SST cycles causes an instantaneous flux that is, with an average of $0.49 \text{ mol C m}^{-2} \text{ yr}^{-1}$, considerably larger in magnitude (absolute value) at WHOTS than at Kilo Nalu. This is a result of the greater gas transfer velocity at higher wind speeds (Wanninkhof, 1992; Nightingale et al., 2000a,b; Ho et al., 2006). Nonetheless, the net annual area specific air-sea CO₂ flux at WHOTS remains small, because summer and winter changes mostly cancel out.

Local Drivers of Air-Sea CO₂ Fluxes

On the south shore, despite larger variability in $p\text{CO}_{2\text{sw}}$ at the Ala Wai site, the overall area specific air-sea CO₂ flux was close to zero at both Ala Wai and Kilo Nalu locations (**Tables 2, 3**). The CRIMP-2 site in Kaneohe Bay, on the other hand, has been a persistent, albeit variable, annual source of CO₂ to the atmosphere (**Figure 6**). The additional years of data since the compilation of Drupp et al. (2013) also show that the flux from the ocean to the atmosphere at CRIMP-2 has increased since 2012.

Air-sea CO₂ fluxes in coastal waters of O'ahu are consistent with the range previously published for coral reef environments around the world (**Table 3**). The flux at CRIMP-2 is close to the flux of $1.30 \text{ mol C cm}^{-2} \text{ yr}^{-1}$, observed at Hog Reef, Bermuda (Bates et al., 2001), a relatively wide and open water reef. It should be kept in mind that fluxes at CRIMP-2 may be even greater than we calculate here, because the current gas transfer velocity parameterization (k) in the flux calculation (Equation 3) does not account for any enhanced gas exchange due to turbulence over the shallow reef (Ho et al., 2016).

Monthly Air-Sea CO₂ Flux Climatology

The climatological differences in air-sea CO₂ fluxes (**Figure 6**) are determined by both the variabilities in $\Delta p\text{CO}_2$ and in wind speed. A clear seasonal cycle is visible at all sites, with more positive fluxes during the summer (outgassing), and smaller or negative fluxes (ingassing) during the winter. This seasonal cycle in air-sea CO₂ fluxes is largely driven by the seasonal $p\text{CO}_{2\text{sw}}$ cycle that determines the $\Delta p\text{CO}_2$ values. At CRIMP-2, the monthly mean CO₂ flux is positive throughout the year and more than an order of magnitude greater than that at the South Shore

TABLE 3 | Area specific air-sea CO₂ fluxes in units of $\text{mol C m}^{-2} \text{ yr}^{-1}$ in tropical and subtropical coral reef environments.

Location	Mean annualized flux ($\text{mol C m}^{-2} \text{ year}^{-1}$)	References
CRIMP-2 (Kaneohe Bay, O'ahu, Hawai'i)	1.14	This work; Drupp et al., 2013
Southern Kaneohe Bay, O'ahu, Hawai'i	1.80	Massaro et al., 2012
Kaneohe Bay, O'ahu, Hawai'i	1.45	Fagan and Mackenzie, 2007
Ala Wai (Mamala Bay, O'ahu, Hawai'i)	0.05	This work; Drupp et al., 2013
Kilo Nalu (Mamala Bay, O'ahu, Hawai'i)	0.01	This work; Drupp et al., 2013
Hog Reef, Bermuda	1.2	Bates et al., 2001
Okinawa Reef flat, Japan	1.8	Ohde and van Woessik, 1999
Yonge Reef, N. Great Barrier Reef, Australia	1.5	Frankignoulle et al., 1996; Gattuso et al., 1996
Moorea, French Polynesia	0.1	Gattuso et al., 1993, 1996, 1997; Frankignoulle et al., 1996
Heron Island, Great Barrier Reef, Australia	0.9	Cyronak et al., 2014
Rarotonga, Cook Islands	3.2	Cyronak et al., 2014
Yongxing Island Reef atoll, Nansha Islands, South China Sea	0.1	Yan et al., 2011
Yongxing Island, Nansha Islands, South China Sea	1.7	Yan et al., 2011
Luhuitou Fringing Reef, South China Sea	3.6	Yan et al., 2011

A positive value indicates a source of CO₂ to the atmosphere.

buoys. There are also clear seasonal differences. The variability in fluxes is greatest in the summer, when the highest $p\text{CO}_{2\text{sw}}$ is observed and trade winds are strong and nearly consistent. During the winter, especially in December and January, wind speed is generally lower and less consistent, and these months are characterized by smaller and less variable fluxes. At Ala Wai and Kilo Nalu, the monthly mean CO₂ fluxes are negative during the winter, and positive during the summer. The greatest variability also coincides with the months characterized by the largest fluxes. The largest positive fluxes are observed in the summer, between August and October, during periods of maximum SST and wind speed. The most negative fluxes, as well as the largest variability in winter months, are observed in February (Kilo Nalu) and March (Ala Wai). This is when strong rains and increased runoff, as well as occasional strong onshore winds, are the most frequent. The presence of riverine input from the Ala Wai Canal results in clear climatological differences in $p\text{CO}_{2\text{sw}}$ at the Ala Wai buoy relative to Kilo Nalu, but this difference is not as evident in the air-sea CO₂ fluxes. The CO₂ flux at WHOTS is negative in winter and positive in summer, and the greatest flux variability at this site is also observed when the flux is the strongest, around

March, similar to what is observed at the South Shore sites (Ala Wai and Kilo Nalu).

Inter-annual Changes in $p\text{CO}_2\text{sw}$

Although the multi-year record obtained at the O'ahu MAPCO₂ buoy network is too short to identify reliably long-term global climate change signals such as OA (Sutton et al., 2019), especially considering the low signal-to-noise ratio in highly variable coastal environments such as the coral reefs around O'ahu, it does allow one to make year to year comparisons and begin to identify inter-annual changes. On an inter-annual timescale, $p\text{CO}_2\text{sw}$ could be affected by climate change, or by climate oscillations such as the El Niño-Southern Oscillation (ENSO). These oscillations drive changes in ocean-atmosphere circulation patterns, as well as SST. They can affect biological productivity and calcification, and therefore should also affect $p\text{CO}_2\text{sw}$ (e.g. Alexander et al., 2002).

Seawater at both our coastal buoys (Ala Wai, Kilo Nalu, and CRIMP-2), and the open ocean WHOTS site, experienced rising maxima in weekly mean seawater temperatures between 2013 and 2015 (Figure 3C). Additionally, all sites display increasing $p\text{CO}_2\text{sw}$ over our time series, which is, however, not statistically significant (7.5 ± 1.9 , 8.3 ± 1.0 , 2.5 ± 0.7 , 2.9 ± 0.6 ppm yr⁻¹ at CRIMP-2, Ala Wai, and Kilo Nalu, and WHOTS respectively; Figures 3A, 8). The increase at Ala Wai is greatest, but this is largely due to the limited dataset, with the anomalously high $p\text{CO}_2\text{sw}$ in the winter of 2013/2014, as discussed above, driving the (apparent) large annual increase. Raw data from more recent deployments at Ala Wai show that *in situ* and weekly mean $p\text{CO}_2\text{sw}$ have since decreased to approximately their previous magnitude (data not shown). This discussion will therefore focus on the CRIMP-2 site, which experienced a very large sustained increase in $p\text{CO}_2\text{sw}$ between 2013 and 2015, and a dramatic increase in the seasonal amplitude of $p\text{CO}_2\text{sw}$ in 2014/2015 to twice the amount observed in 2011 (Figure 3).

Due to the extreme variability in $p\text{CO}_2\text{sw}$ on all temporal scales, it is difficult to isolate possible effects of longer-term signals. To disentangle contributions of different timescales of $p\text{CO}_2\text{sw}$ variability at CRIMP-2, magnitudes of sub-monthly, sub-annual and sub-decadal variability were determined (Table 4). The amplitude of sub-monthly variations, which include diurnal changes from P/R and calcification/dissolution, and fluctuations associated with the effects of mixed tides on time scales of a few hours to 28 days, is the largest (78 μatm). Sub-annual and sub-decadal variability are 34 and 31 μatm , respectively. The main signal on the sub-annual time scale is the seasonal cycle. Consequently, the difference in $p\text{CO}_2\text{sw}$

between the first 4-year period and the second 4-year period of the CRIMP-2 time series has approximately the same magnitude as its average seasonal cycle.

To investigate the potential contribution of climatic oscillations to these sub-decadal variations, annual mean $p\text{CO}_2\text{sw}$ was plotted (Figure 8) with annual mean values of three predominant climate oscillation indices in the North Pacific; the El Niño Southern Oscillation (Oceanic Niño Index, ONI), Pacific Decadal Oscillation (PDO index), and the North Pacific Gyre Oscillation (NPGO index). Correlations between annual mean $p\text{CO}_2\text{sw}$ and ENSO, PDO and NPGO were $R = 0.40$, $R = 0.69$, $R = -0.81$, respectively ($p < 0.01$), suggesting some control of $p\text{CO}_2\text{sw}$ from large-scale climate oscillations.

Changes in physical forcings such as climate oscillations can have an effect on the CO₂ chemistry of seawater on reefs, as has been observed in the open ocean and on coral reefs of Bermuda (Yeakel et al., 2015). A portion of the increase in $p\text{CO}_2\text{sw}$ at CRIMP-2 is also likely due to rising atmospheric CO₂ concentrations from anthropogenic carbon emissions, and penetration of this CO₂ into the surface ocean via air-sea gas exchange, as well as reduced outgassing during natural outgassing periods due to a smaller air-sea gradient. An additional fraction of the sub-decadal $p\text{CO}_2\text{sw}$ variability can likely be explained by the direct temperature effect on CO₂ solubility, which leads to higher (lower) $p\text{CO}_2\text{sw}$ at higher (lower) temperatures.

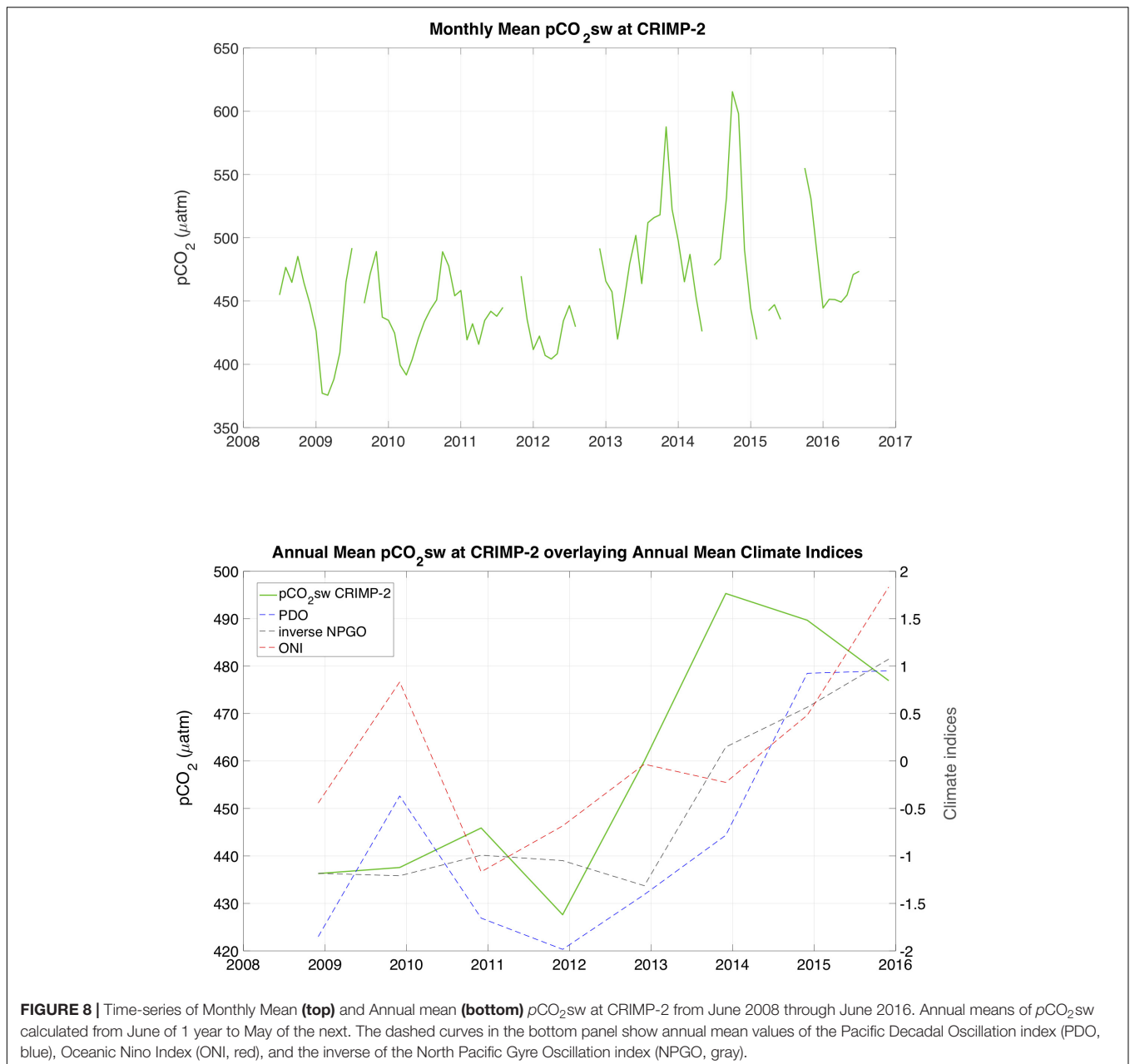
Temperature change and associated $p\text{CO}_2\text{sw}$ change may be driven partly by large scale inter-annual processes such as the ENSO. El Niño events are characterized by larger seasonal amplitudes in SST, while La Niña events have smaller amplitudes. The temperature effect on CO₂ solubility translates this pattern from SST to $p\text{CO}_2\text{sw}$. The period from 2009 to 2010 was classified as a moderate El Niño event⁸, and displays large SST swings, with a lower winter minimum and a higher summer maximum than subsequent years. The periods 2010–2011 and 2011–2012 were identified as moderate and weak La Niña events, respectively, and were characterized by relatively high winter and low summer SST, leading to smaller seasonal fluctuations in SST. The very strong El Niño in winter 2015 to 2016 shows the largest seasonal amplitude, as well as the highest SST of our dataset.

An additional factor in explaining rising SST between 2013 and 2016 is the North Pacific warm pool, a positive basin-wide SST anomaly beginning in the winter of 2013–2014 (Peterson et al., 2015). Sutton et al. (2017) also proposed that elevated seawater $p\text{CO}_2\text{sw}$ at the WHOTS buoy during the period 2013–2015 may have been driven by North Pacific warm anomalies, consistent with our observations at CRIMP-2 over a similar time period. Models and observations indicate that the amplitude of diurnal to seasonal $p\text{CO}_2\text{sw}$ variability in the oceans will likely increase with increasing anthropogenic CO₂ uptake (McNeil and Sasse, 2016; Kwiatkowski and Orr, 2018; Landschützer et al., 2018). This factor could lead to increasing prevalence of conditions similar to the higher and more variable $p\text{CO}_2\text{sw}$ regime of 2013–2016 at CRIMP-2.

TABLE 4 | Amplitude of $p\text{CO}_2\text{sw}$ variability at CRIMP-2 on different time scales, defined as the average standard deviation of monthly, annual and 4-year mean $p\text{CO}_2\text{sw}$.

Timescale of variability	$p\text{CO}_2\text{sw}$ (μatm)
Sub-monthly	78
Sub-annual	34
Sub-decadal	31

⁸<http://ggweather.com/enso/oni.htm>



El Niño events are also associated with lower trade wind speeds (Collins et al., 2010, and references therein). Weakening of the trade winds increases the residence time of water on the Kaneohe Bay reef flat (e.g., Lowe et al., 2009b) and also reduces air-sea gas exchange rates (e.g., Wanninkhof, 1992; Ho et al., 2006, 2019). Thus, both increased residence time and decreased air-sea gas exchange lead to a stronger buildup of biogeochemical signatures of primary productivity and dissolution (drawdown of pCO₂sw) and respiration and calcification (increase in pCO₂sw), respectively. Weaker trade winds are therefore likely partially responsible for the greater amplitude of fluctuations in pCO₂sw at CRIMP-2 during El Niño years.

Changes in biogeochemical processes on the reef that could cause an increase in pCO₂sw at CRIMP-2 between 2013 and 2016 include: (1) an increase in net ecosystem calcification (NEC) (e.g., Drupp et al., 2013; Courtney et al., 2017) and (2) an increase in respiration of organic matter relative to primary production (e.g., Drupp et al., 2011, 2013). An increase in NEC seems unlikely. The high SST during the summers of 2014 and 2015 caused widespread coral bleaching throughout the Hawaiian Islands, and led to lower calcification rates on the barrier reef of Kaneohe Bay. The reefs largely recovered by Courtney et al. (2017). An increase of respiration on the reef flat, however, is more likely responsible for the observed higher pCO₂sw between 2012

and 2016. Rates of biogeochemical processes typically increase with increasing (seawater) temperature, but respiration is more sensitive to temperature changes than primary production (“Q10 effect,” e.g., Woodwell and Mackenzie, 1995; Ver et al., 1999). Higher SST consequently causes enhanced respiration relative to photosynthesis, which increases $p\text{CO}_2\text{sw}$. The barrier reef ecosystem is perhaps shifting toward longer periods of heterotrophy as a result of elevated SST between 2013 and 2016. Photosynthesis/respiration cycles appear to be a more important

driver of $p\text{CO}_2\text{sw}$ at CRIMP-2 than calcification/dissolution (see Page et al., 2018). Therefore, the relative increase in the ratio of respiration to photosynthesis likely outweighs the decrease in $p\text{CO}_2\text{sw}$ due to lower calcification, resulting in higher $p\text{CO}_2\text{sw}$ values during periods of temperature-induced coral bleaching. Kayanne et al. (2005) also measured an increase in $p\text{CO}_2\text{sw}$ in coral reefs with extensive bleaching, but observed a concomitant 50% decrease in diurnal variability associated with reduced metabolic performance. This does not apply to the bleaching

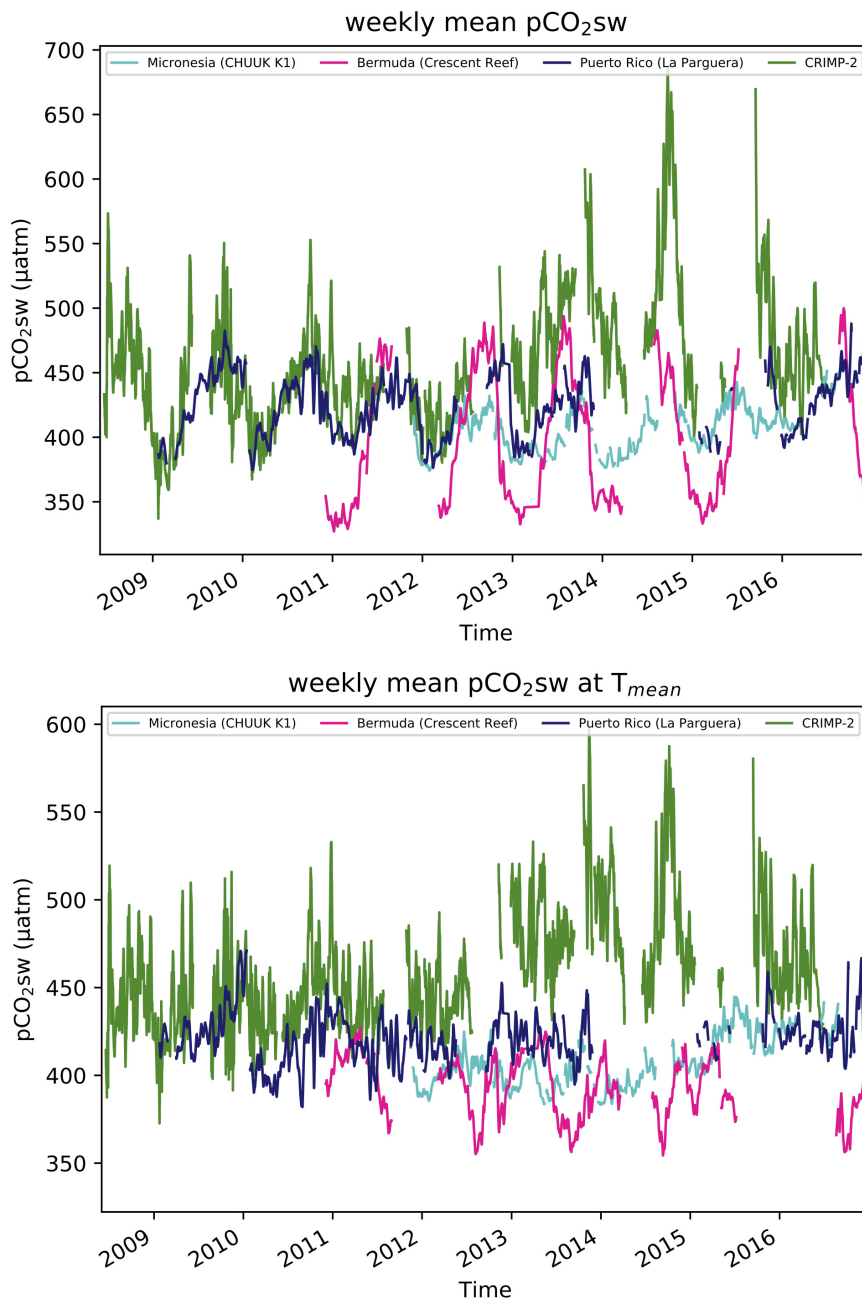


FIGURE 9 | Time-series of weekly mean $p\text{CO}_2\text{sw}$ (**Top**) and temperature normalized $p\text{CO}_2\text{sw}$ ($p\text{CO}_2\text{sw}$ at T_{mean} , **Bottom**) at different reef sites for June 2008 through December 2016.

period in Kaneohe Bay, where CRIMP-2 diurnal variability did not decrease.

The $p\text{CO}_2\text{sw}$ increase observed at CRIMP-2 was greater than those observed at MAPCO₂ sites at coral reefs in different parts of the world (Figure 9 and online⁹). The records from La Parguera site, on the southwestern coast of Puerto Rico, and CRIMP-2 nearly overlap early (2009) in the time series: The maxima in summer are roughly 50 ppm higher at CRIMP-2, but the means and amplitudes are comparable. The similarity in the CRIMP-2 and La Parguera $p\text{CO}_2\text{sw}$ records disappears after the winter of 2011–2012, when $p\text{CO}_2\text{sw}$ at CRIMP-2 begins to rise considerably. Neither the Chuuk K1 site, a low latitude (7.5°N) reef in Micronesia, or the Crescent reef site in Bermuda showed a significant trend in $p\text{CO}_2\text{sw}$, or a baseline shift similar to the CRIMP-2 observations. Upon normalization to the overall mean temperature (Figure 8) at each site over the respective time periods, $p\text{CO}_2\text{sw}$ at both moorings in tropical waters of the Pacific (CRIMP-2 and Chuuk K1) appears to rise toward the end of the time series, while $p\text{CO}_2\text{sw}$ at T_{mean} at La Parguera and Crescent reef do not exhibit the same feature.

The observed similarity between both North Pacific reefs in temperature normalized $p\text{CO}_2\text{sw}$ may be attributed partially to the influence of basin wide changes in physical processes, such as SST and wind speed variations. The larger variability of $p\text{CO}_2\text{sw}$ at CRIMP-2 relative to other reefs around the world, however, is likely driven more by local changes in biogeochemistry on the Kaneohe Bay barrier reef, which are themselves influenced strongly by inter-annual changes in large scale ocean-atmosphere circulation patterns. The relative importance of these drivers can only be assessed with additional years of continuous monitoring that can resolve the time scales of inter-annual variability and long-term trends.

CONCLUSION

In this paper we presented a statistical evaluation and interpretation of nearly a decade of high-resolution CO₂ time-series data collected between June 2008 and December 2016 at three different coral reef environments off the island of O'ahu, Hawai'i. Our major findings are:

- Land-ocean interactions, water column and benthic photosynthesis/respiration and calcification/dissolution, as well as physical forcing (wind, waves, and water residence time), all exert controls on $p\text{CO}_2\text{sw}$ and air-sea CO₂ fluxes, which are therefore more variable on coral reefs than in the open ocean.
- Diurnal $p\text{CO}_2\text{sw}$ variability was, on average, 40 times greater on the Kaneohe Bay barrier reef than in waters of the North Pacific subtropical gyre, and comparatively less so (10 times) at the more exposed fringing reef sites of O'ahu, driven largely by daily cycles of photosynthesis

and respiration. The temperature effect on CO₂ solubility is the largest driver of seasonal $p\text{CO}_2\text{sw}$ variability, with additional impacts by biogeochemical processes that differ between reef locations.

- While seasonal variability determines the direction of air-sea CO₂ fluxes in the open ocean, which are negative in winter (sink for atmospheric CO₂) and positive in summer, large short-term changes occur in coastal coral reef systems. Instantaneous air-sea CO₂ fluxes on O'ahu's coral reefs are highly variable in magnitude and direction and, reflecting local dynamic conditions, often switch between being a source or a sink of CO₂ on timescales of hours to days. Overall estimated area specific air-sea CO₂ fluxes at CRIMP-2, Ala Wai and Kilo Nalu sites of 1.24, 0.05, 0.00 mol C m⁻²yr⁻¹, respectively, are consistent with earlier work, indicating that the productive coral reefs of Hawai'i are generally a source of CO₂ to the atmosphere.
- Instantaneous air-sea CO₂ fluxes were most variable during the summer at CRIMP-2 due to higher SST enhancing biological productivity. At the south shore sites, on the other hand, the variability was greater in winter and spring, likely due to increased rainfall delivering nutrients to the coastal ocean.
- Relatively low peak $p\text{CO}_2\text{sw}$ at CRIMP-2 in the early parts of our time-series (2008 and 2010) coincided with La Niña periods, whereas higher peak $p\text{CO}_2\text{sw}$ later in our time series (2014–2016) coincided with El Niño.
- The observed inter-annual increase in $p\text{CO}_2\text{sw}$ at CRIMP-2 over the study period may reflect the influence of climate oscillations on local conditions: Firstly, increased seawater temperature both directly increases $p\text{CO}_2\text{sw}$ and may enhance rates of respiration, which also increase $p\text{CO}_2\text{sw}$. Secondly, reduced trade wind speed increases the water residence time on the reef, allowing for more build-up of CO₂ in seawater.
- Variability in $p\text{CO}_2\text{sw}$ at CRIMP-2 is greatest at timescales shorter than a month (78 μatm), while average seasonal and inter-annual variations are 34 and 31 μatm, respectively. Consequently, there is a large magnitude of short-term changes due to reef metabolism and physical drivers overlaying a smaller amplitude seasonal cycle, and comparable inter-annual changes on a time-scale of approximately 5 years. This shows that inter-annual changes in $p\text{CO}_2$ are difficult to identify on a background of extremely large shorter-term variability at CRIMP-2.

AUTHOR CONTRIBUTIONS

GT, PD, EDC, FM, and CS contributed to the conception and design of the study. GT and EDC wrote an earlier version of the manuscript. LK and GT re-wrote the manuscript, performed statistical analysis, and generated figures and tables. AS and AP contributed to datasets. YL provided valuable insights into interpretations of the data. All authors contributed to manuscript revisions, read and approved the submitted version.

⁹<http://www.pmel.noaa.gov/co2/story/Coral+Reef+Moorings>

FUNDING

We acknowledge with gratitude the financial support of our research provided in part by a grant/cooperative agreement from the National Oceanic and Atmospheric Administration, Project R/IR-27, which is sponsored by the University of Hawaii Sea Grant College Program, SOEST, under Institutional Grant No. NA14OAR4170071 from NOAA Office of Sea Grant, Department of Commerce. Additional support was granted by the NOAA/Ocean Acidification Program (to EDC and AS) and the NOAA/Climate Program Office (AP), and the NOAA Ocean Observing and Monitoring Division, Climate Program Office (FundRef number 100007298) through agreement NA14OAR4320158 of the NOAA Cooperative Institute for the North Atlantic Region (AP). The views expressed herein are those of the author(s) and do not necessarily reflect the views of NOAA or any of its subagencies. This is SOEST contribution number 10684,

REFERENCES

- Alexander, M. A., Blade, I., Newman, M., Lanzante, J. R., Lau, N. C., and Scott, J. D. (2002). The atmospheric bridge: the influence of ENSO teleconnections on air–sea interaction over the global oceans. *J. Clim.* 15, 2205–2231. doi: 10.1175/1520-0442(2002)015<%3C2205%3AAtabtio%3E2.0.co%3B2
- Andersson, A. J., and Gledhill, D. (2013). Ocean acidification and coral reefs: effects on breakdown, dissolution, and net ecosystem calcification. *Annu. Rev. Mar. Sci.* 5, 321–348. doi: 10.1146/annurev-marine-121211-172241
- Bates, N. R., Astor, Y. M., Church, M. J., Currie, K., Dore, J. E., González-Dávila, M., et al. (2014). A time-series view of changing ocean chemistry due to ocean uptake of anthropogenic CO₂ and ocean acidification. *Oceanography* 27, 126–141. doi: 10.5670/oceanog.2014.16
- Bates, N. R., Samuels, L., and Merlivat, L. (2001). Biogeochemical and physical factors influencing seawater *f*CO₂ and air–sea CO₂ exchange on the Bermuda coral reef. *Limnol. Oceanogr.* 46, 833–846. doi: 10.4319/lo.2001.46.4.0833
- Caldeira, K., and Wickett, M. E. (2003). Oceanography: anthropogenic carbon and ocean pH. *Nature* 425, 365–365. doi: 10.1038/425365a
- Chamard, P., Thiery, F., Di Sarra, A., Ciattaglia, L., De Silverstri, L., Grigioni, P., et al. (2003). Interannual variability of atmospheric CO₂ in the mediterranean: measurements at the island of Lampedusa. *Tellus* 55, 83–93. doi: 10.1034/j.1600-0889.2003.00048.x
- Chhak, K. C., and Di Lorenzo, E. (2009). Forcing of low-frequency ocean variability in the Northeast Pacific*. *J. Clim.* 22, 1255–1276. doi: 10.1175/2008jcli2639.1
- Collins, M., An, S. I., Cai, W., Ganachaud, A., Guilyardi, E., Jin, F. F., et al. (2010). The impact of global warming on the tropical Pacific Ocean and El Niño. *Nat. Geosci.* 3, 391–397.
- Courtney, T., De Carlo, E. H., Page, H. N., Bahr, K. D., Barro, A., Howins, N., et al. (2017). Recovery of reef-scale calcification following a bleaching event in Kaneohe Bay, Hawai'i. *Limnol. Oceanogr. Lett.* 3, 1–9. doi: 10.1002/lo.21005
- Cyronak, T., Santos, I. R., Erler, D. V., Maher, D. T., and Eyre, B. D. (2014). Drivers of pCO₂ variability in two contrasting coral reef lagoons: the influence of submarine groundwater discharge. *Global Biogeochem. Cycles* 28, 398–414. doi: 10.1002/2013gb004598
- De Carlo, E. H., Beltran, V. L., and Tomlinson, M. S. (2004). Composition of water and suspended sediment in streams of urbanized subtropical watersheds in Hawaii. *Appl. Geochem.* 19, 1011–1037. doi: 10.1016/j.apgeochem.2004.01.004
- De Carlo, E. H., Hoover, D. J., Young, C. W., Hoover, R. S., and Mackenzie, F. T. (2007). Impact of storm runoff from tropical watersheds on coastal water quality and productivity. *Appl. Geochem.* 22, 1777–1797. doi: 10.1016/j.apgeochem.2007.03.034
- PMEL contribution number 4845, and Hawai'i Sea Grant contribution UNIHI-SEAGRANT-JC-15-30.

ACKNOWLEDGMENTS

We are grateful to research groups working on NOAA MAPCO₂ moorings globally who supplied data for comparison: the Korea Institute of Ocean Science and Technology (Chuuk K1), University of Puerto Rico (La Parguera), and the Bermuda Institute of Ocean Science (Crescent Reef). We would like to thank Ryan Tabata, Noah Howins, and Anthony Barro (at UH), as well as Sylvia Musielewicz, Stacy Maenner-Jones, and Randy Bott (at NOAA/PMEL) who provided technical support and their efforts are deeply appreciated as this research would not have been possible without their able assistance. This manuscript also benefited from reviews from several reviewers who helped improve the quality of this manuscript.

- Di Lorenzo, E., Schneider, N., Cobb, K. M., Franks, P. J. S., Chhak, K., Miller, A. J., et al. (2008). North Pacific gyre oscillation links ocean climate and ecosystem change. *Geophys. Res. Lett.* 35:L08607. doi: 10.1111/gcb.13171
- Dlugokencky, E., and Tans, P. (2018). *Trends in Atmospheric Carbon Dioxide*. NOAA/ESRL. Available at: <http://www.esrl.noaa.gov/gmd/ccgg/trends/global.html> (accessed April 17, 2019).
- Dore, J. E., Lucas, R., Sadler, D. W., Church, M. J., and Karl, D. M. (2009). Physical and biogeochemical modulation of ocean acidification in the central North Pacific. *PNAS* 106, 12235–12240. doi: 10.1073/pnas.0906044106
- Dore, J. E., Lukas, R., Sadler, D. W., and Karl, D. M. (2003). Climate-driven changes to the atmospheric CO₂ sink in the subtropical North Pacific Ocean. *Nature* 424, 754–757. doi: 10.1038/nature01885
- Drupp, P., De Carlo, E. H., Mackenzie, F. T., Bienfang, P., and Sabine, C. L. (2011). Nutrient inputs, phytoplankton response, and CO₂ variations in a semi-enclosed subtropical embayment, Kaneohe Bay, Hawaii. *Aquat. Geochem.* 17, 473–498. doi: 10.1007/s10498-010-9115-y
- Drupp, P. S., De Carlo, E. H., and Mackenzie, F. T. (2016). Porewater CO₂-carbonic acid geochemistry in sandy sediments. *Mar. Chem.* 185, 48–64. doi: 10.1016/j.marchem.2016.04.004
- Drupp, P. S., DeCarlo, E. H., Mackenzie, F. T., Sabine, C. L., Feely, R. A., and Shamberger, K. E. (2013). Comparison of CO₂ dynamics and air–sea gas exchange in differing tropical reef environments. *Aquat. Geochem.* 19, 371–397. doi: 10.1007/s10498-013-9214-7
- Eyre, B., Cyronak, T., Drupp, P., De Carlo, E. H., Sachs, J., and Andersson, A. J. (2018). Coral reefs will transition to net dissolving before end of century. *Science* 359, 908–911. doi: 10.1126/science.aao1118
- Fagan, K. E., and Mackenzie, F. T. (2007). Air–sea CO₂ exchange in a subtropical estuarine-coral reef system, Kaneohe Bay, Oahu, Hawaii. *Mar. Chem.* 106, 174–191. doi: 10.1016/j.marchem.2007.01.016
- Feely, R. A., Sabine, C. L., Lee, K., Berelson, W., Kleyvas, J., Fabry, V. J., et al. (2004). Impact of anthropogenic CO₂ on the CaCO₃ system in the oceans. *Science* 305, 362–366. doi: 10.1126/science.1097329
- Frankignoulle, M., Gattuso, J. P., Biondo, R., Bourge, I., Copin-Montégut, G., and Pichon, M. (1996). Carbon fluxes in coral reefs. II. Eulerian study of inorganic carbon dynamics and measurement of air–sea CO₂ exchanges. *Mar. Ecol. Prog. Ser.* 145, 123–132. doi: 10.3354/meps145123
- Fogaren, K. E., Sansone, F. J., and De Carlo, E. H. (2013). Porewater temporal variability in a wave-impacted permeable nearshore sediment. *Mar. Chem.* 149, 74–84. doi: 10.1016/j.marchem.2012.12.005
- Gagliano, M., McCormick, M. I., Moore, J. A., and Depczynski, M. (2010). The basics of acidification: baseline variability of pH on Australian coral reefs. *Mar. Biol.* 157, 1849–1856. doi: 10.1007/s00227-010-1456-y
- Gattuso, J. P., and Hansson, L. (2011). *Ocean Acidification*. Oxford: Oxford University Press.

- Gattuso, J.-P., Payri, C. E., Pichon, M., Delesalle, B., and Frankignoulle, M. (1997). Primary production, calcification, and air-sea CO₂ fluxes of a macroalgal-dominated coral reef community in Moorea, French Polynesia. *J. Phycol.* 33, 729–738. doi: 10.1111/j.0022-3646.1997.00729.x
- Gattuso, J. P., Pichon, M., Delesalle, B., Canon, C., and Frankignoulle, M. (1996). Carbon fluxes in coral reefs. I. Lagrangian measurement of community metabolism and resulting air-sea CO₂ disequilibrium. *Mar. Ecol. Prog. Ser.* 145, 109–121. doi: 10.3354/meps145109
- Gattuso, J.-P., Pichon, M., Delesalle, B., and Frankignoulle, M. (1993). Community metabolism and air-sea CO₂ fluxes in a coral-reef ecosystem (Moorea, French-Polynesia). *Mar. Ecol. Prog. Ser.* 96, 259–267. doi: 10.3354/meps096259
- Giambelluca, T. W., Chen, Q., Frazier, A. G., Price, J. P., Chen, Y.-L., Chu, P. S., et al. (2011). *The Rainfall Atlas of Hawai'i*. Available at: <http://rainfall.geography.hawaii.edu> (accessed April 17, 2019).
- Giambelluca, T. W., Nullet, M. A., and Schroeder, T. A. (1986). *Rainfall atlas of Hawaii*. Hawaii, HI: Department of Land and Natural Resources.
- Ho, D., De Carlo, E. H., and Schlosser, P. (2019). Air-sea gas exchange and CO₂ fluxes in a tropical coral reef lagoon. *J. Geophys. Res. Oceans* 123, 8701–8713. doi: 10.1029/2018JC014423
- Ho, D. T., Coffineau, N., Hickman, B., Chow, N., Koffman, T., and Schlosser, P. (2016). Influence of current velocity and wind speed on air-water gas exchange in a mangrove estuary. *Geophys. Res. Lett.* 43, 3813–3821. doi: 10.1002/2016gl068727
- Ho, D. T., Law, C. S., Smith, M. J., Schlosser, P., Harvey, M., and Hill, P. (2006). Measurements of air-sea gas exchange at high wind speeds in the Southern Ocean: implications for global parameterization. *Geophys. Res. Lett.* 33:L16611 doi: 10.1029/2006GL026817
- Hoegh-Guldberg, O., Mumby, P. J., Hooten, A. J., Steneck, R. S., Greenfield, P., Gomez, E., et al. (2007). Coral reefs under rapid climate change and ocean acidification. *Science* 318, 1737–1742.
- Hofmann, G. E., Smith, J. E., Johnson, K. S., Send, U., Levin, L. A., Micheli, F., et al. (2011). High-frequency dynamics of ocean pH: a multi-ecosystem comparison. *PLoS One* 6:e28983. doi: 10.1371/journal.pone.0028983
- Hoover, D. J., and Mackenzie, F. T. (2009). Fluvial fluxes of water, suspended particulate matter, and nutrients and potential impacts on tropical coastal water biogeochemistry: Oahu, Hawaii. *Aquat. Geochem.* 15, 547–570. doi: 10.1007/s10498-009-9067-2
- Hoover, R. S., Hoover, D., Miller, M., Landry, M. R., DeCarlo, E. H., and Mackenzie, F. T. (2006). Zooplankton response to storm runoff in a tropical estuary: bottom-up and top-down controls. *Mar. Ecol. Prog. Ser.* 318, 187–201. doi: 10.3354/meps318187
- Karl, D. M., and Church, M. J. (2018). Station ALOHA: a gathering place for discovery, education, and scientific collaboration. *Limnol. Oceanogr. Bull.* 28, 10–12. doi: 10.1002/lob.10285
- Kayanne, H., Hata, H., Kudo, S., Yamano, H., Watanabe, A., Ikeda, Y., et al. (2005). Seasonal and bleaching-induced changes in coral reef metabolism and CO₂ flux. *Global Biogeochem. Cycles* 19. doi: 10.1029/2004GB002400
- Kayanne, H., Suzuki, A., and Saito, H. (1995). Diurnal changes in the partial pressure of carbon dioxide in coral reef water. *Science* 269, 214–216. doi: 10.1126/science.269.5221.214
- Keeling, C. D., Bacastow, R. B., Bainbridge, A. E., Ekdahl, C. A., Guenther, P. R., and Waterman, L. S. (1976). Atmospheric carbon dioxide variations at Mauna Loa Observatory, Hawaii. *Tellus* 28, 538–551. doi: 10.3402/tellusa.v28i6.11322
- Keeling, C. D., Piper, S. C., Bacastow, R. B., Wahlen, M., Whorf, T. P., Heimann, M., et al. (2001). *Exchanges of Atmospheric CO₂ and 13CO₂ with the Terrestrial Biosphere and Oceans from 1978 to 2000. I. Global Aspects, SIO Reference Series, No. 01-06*. San Diego, CA: Scripps Institution of Oceanography.
- Kleypas, J. A., Buddemeier, R. W., Archer, D., Gattuso, J. P., Langdon, C., and Opdyke, B. N. (1999). Geochemical consequences of increased atmospheric carbon dioxide on coral reefs. *Science* 284, 118–120. doi: 10.1126/science.284.5411.118
- Kleypas, J. A., and Langdon, C. (2006). “Coral Reefs and changing seawater carbonate chemistry,” in *Coral Reefs and Climate Change: Science and Management*, eds J. T. Phinney, O. Hoegh-Guldberg, J. Kleypas, W. Skirving, and A. Strong (Washington, DC: American Geophysical Union), doi: 10.1029/61CE06
- Kwiatkowski, L., and Orr, J. C. (2018). Diverging seasonal extremes for ocean acidification during the twenty-first century. *Nat. Clim. Change* 8, 141–145. doi: 10.1038/s41558-017-0054-0
- Landschützer, P., Gruber, N., Bakker, D. C. E., Stemmler, I., and Six, K. D. (2018). Strengthening seasonal marine CO₂ variations due to increasing atmospheric CO₂. *Nat. Clim. Change* 8, 146–150. doi: 10.1038/s41558-017-0057-x
- Le Quéré, C. L., Andrew, R. M., Friedlingstein, P., Sitch, S., Pongratz, J., Manning, A. C., et al. (2018). Global Carbon Budget 2017. *Earth Syst. Sci. Data* 10, 405–448. doi: 10.5194/essd-10-405-2018
- Liss, P. S. (1983). “Gas transfer: experiments and geochemical implications,” in *Air-Sea Exchange of Gases and Particles*, eds P. S. Liss and W. G. N. Slinn (Dordrecht: D. Reidel), 241–298. doi: 10.1007/978-94-009-7169-1_5
- Lowe, R. J., Falter, J. L., Monismith, S. G., and Atkinson, M. J. (2009a). A numerical study of circulation in a coastal reef-lagoon system. *J. Geophys. Res. Oceans* 114:C06022.
- Lowe, R. J., Falter, J. L., Monismith, S. G., and Atkinson, M. J. (2009b). Wave-driven circulation of a coastal reef-lagoon system. *J. Phys. Oceanogr.* 39, 873–889.
- Mackenzie, F. T., and Andersson, A. J. (2013). The marine carbon system and ocean acidification during Phanerozoic time. *Geochem. Perspect.* 2, 1–3.
- Massaro, R. F., De Carlo, E. H., Drupp, P. S., Mackenzie, F. T., Maenner Jones, S., Shamberger, K. E., et al. (2012). Multiple factors driving variability of CO₂ exchange between the ocean and atmosphere in a tropical coral reef environment. *Aquat. Geochem.* 18, 357–386. doi: 10.1007/s10498-012-9170-7
- McNeil, B. I., and Sasse, T. P. (2016). Future ocean hypercapnia driven by anthropogenic amplification of the natural CO₂ cycle. *Nature* 529, 383–386. doi: 10.1038/nature16156
- Nightingale, P. D., Liss, P. S., and Schlosser, P. (2000a). Measurements of air-sea gas transfer during an open ocean algal bloom. *Geophys. Res. Lett.* 27, 2117–2120. doi: 10.1029/2000gl011541
- Nightingale, P. D., Malin, G., Law, C. S., Watson, A. J., Liss, P. S., Liddicoat, M. I., et al. (2000b). In situ evaluation of air-sea gas exchange parameterizations using novel conservative and volatile tracers. *Glob. Biogeochem. Cycles* 14, 373–387. doi: 10.1029/1999gb900091
- Ohde, S., and van Woesik, R. (1999). Carbon dioxide flux and metabolic processes of a coral reef, Okinawa. *Bull. Mar. Sci.* 65, 559–576.
- Page, H. N., Courtney, T. A., Collins, A., De Carlo, E. H., and Andersson, A. J. (2017). Net community metabolism and seawater carbonate chemistry scale non-intuitively with coral cover. *Front. Mar. Sci.* 4:161. doi: 10.3389/fmars.2017.00161
- Page, H. N., Courtney, T. A., De Carlo, E. H., Howins, N., Koester, I., and Andersson, A. J. (2018). Spatio-temporal variability in seawater carbon chemistry for a coral reef flat in Kaneohe Bay, Hawaii. *Limnol. Oceanogr.* 9999, 1–22. doi: 10.1002/lno.11084
- Peterson, E. W., and Hennessey, J. P. (1978). On the use of power laws for estimates of wind power potential. *J. Appl. Meteorol.* 17, 390–394. doi: 10.1175/1520-0450(1978)017%3C0390%3Aotuoapl%3E2.0.co%3B2
- Peterson, W., Robert, M., and Bond, N. (2015). The warm blob-conditions in the northeastern Pacific Ocean. *North Pac. Mar. Sci. Organ.* 23, 36–38.
- Price, N. N., Martz, T. R., Brainard, R. E., and Smith, J. E. (2012). Diel variability in seawater pH relates to calcification and benthic community structure on coral reefs. *PLoS One* 7:e43843. doi: 10.1371/journal.pone.0043843
- Ringuef, S., and Mackenzie, F. T. (2005). Controls on nutrient and phytoplankton dynamics during normal flow and storm runoff conditions, Southern Kaneohe Bay, Hawaii. *Estuaries* 28, 327–337. doi: 10.1007/bf02693916
- Sabine, C. L., Feely, R. A., Gruber, N., Key, R. M., Lee, K., Bullister, J. L., et al. (2004). The oceanic sink for anthropogenic CO₂. *Science* 305, 367–371. doi: 10.1126/science.1097403
- Shamberger, K. E., Feely, R. A., Sabine, C. L., Atkinson, M. J., De Caro, E. H., Mackenzie, F. T., et al. (2011). Calcification and organic production on a Hawaiian coral reef. *Mar. Chem.* 127, 64–75. doi: 10.1016/j.marchem.2011.08.003
- Shaw, E. C., and McNeill, B. I. (2014). Seasonal variability in carbonate chemistry and air-sea CO₂ fluxes in the southern Great Barrier Reef. *Mar. Chem.* 158, 49–58. doi: 10.1016/j.marchem.2013.11.007
- Shaw, E., Tilbrook, B., Steven, A., and Phinn, S. (2014). *Carbonate Chemistry, Community Metabolism, PAR, Temperature and Salinity of One Tree Island Reef*. Bremen: Pangaea.

- Sutton, A. J., Feely, R. A., Maenner-Jones, S., Musielwicz, S., Osborne, J., Dietrich, C., et al. (2019). Autonomous seawater pCO₂ and pH time series from 40 surface buoys and the emergence of anthropogenic trends. *Earth Syst. Sci. Data* 11, 421–439. doi: 10.5194/essd-11-421-2019
- Sutton, A. J., Feely, R. A., Sabine, C. L., McPhadden, M. L., Takahashi, T., Chavez, F. P., et al. (2014a). Natural variability and anthropogenic change in equatorial Pacific surface ocean pCO₂ and pH. *Glob. Biogeochem. Cycles* 28, 131–145. doi: 10.1002/2013GB004679
- Sutton, A. J., Sabine, C. L., Feely, R. A., Cai, W. J., Cronin, M. F., McPhaden, M. J., et al. (2016). Using present-day observations to detect when anthropogenic change forces surface ocean carbonate chemistry outside preindustrial bounds. *Biogeosciences* 13, 5065–5083. doi: 10.5194/bg-13-5065-2016
- Sutton, A. J., Sabine, C. L., Maenner-Jones, S., Lawrence-Slavas, N., Meinig, C., Feely, R. A., et al. (2014b). A high-frequency atmospheric and seawater pCO₂ data set from 14 open-ocean sites using a moored autonomous system. *Earth Syst. Sci. Data* 6, 353–366. doi: 10.5194/essd-6-353-2014
- Sutton, A. J., Wanninkhof, R., Sabine, C. L., Feely, R. A., Cronin, M. F., and Weller, R. A. (2017). Variability and trends in surface seawater pCO₂ and CO₂ flux in the Pacific Ocean. *Geophys. Res. Lett.* 44, 5627–5636. doi: 10.1002/2017GL073814
- Takahashi, T., Olafsson, J., Goddard, J. G., Chipman, D. W., and Sutherland, S. C. (1993). Seasonal-variation of CO₂ and nutrients in the high-latitude surface oceans—a comparative study. *Glob. Biogeochem. Cycles* 7, 843–878. doi: 10.1029/93gb02263
- Takahashi, T., Sutherland, S. C., Sweeney, C., Poisson, A., Metz, N., Tilbrook, B., et al. (2002). Global sea–air CO₂ flux based on climatological surface ocean pCO₂, and seasonal biological and temperature effects. *Deep Sea Res. Part 2 Top. Stud. Oceanogr.* 49, 1601–1622. doi: 10.1016/s0967-0645(02)00003-6
- Tans, P. P., and Kielling, R. (2017). NOAA/ESRL. Available at: www.esrl.noaa.gov/gmd/ccgg/trends (accessed April 17, 2019).
- Thoning, K. W., Tans, P. P., and Komhyr, W. D. (1989). Atmospheric carbon dioxide at mauna loa observatory 2. analysis of the NOAA GMCC data, 1974–1985. *J. Geophys. Res.* 94, 8549–8565. doi: 10.1029/jd094id06p08549
- Tokoro, T., Hosokawa, S., Miyoshi, E., Tada, K., Watanabe, K., Montani, S., et al. (2014). Net uptake of atmospheric CO₂ by coastal submerged aquatic vegetation. *Glob. Change Biol.* 20, 1873–1884. doi: 10.1111/gcb.12543
- Tomlinson, M. S., De Carlo, E. H., McManus, M. A., Pawlak, G., and Steward, G. F. (2011). Characterizing the effects of two storms on the coastal waters of Oahu, Hawaii, using data from the Pacific Islands Ocean Observing System. *Oceanography* 24, 182–198.
- Ver, L. M. B., Mackenzie, F. T., and Lerman, A. (1999). Biogeochemical responses of the carbon cycle to natural and human perturbation: past, present, and future. *Am. J. Sci.* 299, 762–801. doi: 10.2475/ajs.299.7-9.762
- Wanninkhof, R. (1992). Relationship between wind speed and gas exchange over the ocean. *J. Geophys. Res.* 97, 7373–7382.
- Weiss, R. F. (1974). Carbon dioxide in water and seawater: the solubility of a non-ideal gas. *Mar. Chem.* 2, 203–215. doi: 10.1016/0304-4203(74)90015-2
- Weiss, R. F., and Price, B. A. (1980). Nitrous oxide solubility in water and seawater. *Mar. Chem.* 8, 347–359. doi: 10.1016/0304-4203(80)90024-9
- Weller, R. A. (2018). “Observing Surface Meteorology and Air-Sea Fluxes,” in *Observing the Oceans in Real Time*, eds R. Venkatesan, A. Tandon, E. D’Asaro, and M. A. Atmanand (New York, NY: Springer Oceanography), 17–35. doi: 10.1007/978-3-319-66493-4_2
- Woodwell, G. M., and Mackenzie, F. T. (1995). *Biotic Feedbacks in the Global Climatic System: Will the Warming Feed the Warming?* New York, NY: Oxford University Press.
- Yan, H., Yu, K., Shi, Q., Tan, Y., Lui, G., Zhao, M., et al. (2016). Seasonal variations of seawater pCO₂ and sea-air CO₂ fluxes in a fringing coral reef, northern South China Sea. *J. Geophys. Res. Oceans* 121, 998–1008. doi: 10.1002/2015jc011484
- Yan, H., Yu, K., Shi, Q., Tan, Y., Zhang, H., Zhao, M., et al. (2011). Coral reef ecosystems in the South China Sea as a source of atmospheric CO₂ in summer. *Chin. Sci. Bull.* 56, 676–684. doi: 10.1007/s11434-011-4372-8
- Yeakel, K. L., Nadersson, A. J., Bates, N. R., Noyes, T. J., Collins, A., and Garley, R. (2015). Shifts in coral reef biogeochemistry and resulting acidification linked to offshore productivity. *PNAS* 112, 14512–14517. doi: 10.1073/pnas.1507021112

Conflict of Interest Statement: The authors declare that the research was conducted in the absence of any commercial or financial relationships that could be construed as a potential conflict of interest.

Copyright © 2019 Terlouw, Knor, De Carlo, Drupp, Mackenzie, Li, Sutton, Plueddemann and Sabine. This is an open-access article distributed under the terms of the Creative Commons Attribution License (CC BY). The use, distribution or reproduction in other forums is permitted, provided the original author(s) and the copyright owner(s) are credited and that the original publication in this journal is cited, in accordance with accepted academic practice. No use, distribution or reproduction is permitted which does not comply with these terms.